Analytical and Bioanalytical Chemistry
https://doi.org/10.1007/s00216-021-03687-9

REVIEW

The latest advances on nonlinear insulator-based electrokinetic microsystems under direct current and low-frequency alternating current fields: a review

Blanca H. Lapizco-Encinas[1]

Received: 5 July 2021 / Revised: 17 September 2021 / Accepted: 21 September 2021

Abstract

This review article presents an overview of the evolution of the field of insulator-based dielectrophoresis (iDEP); in particular, it focuses on insulator-based electrokinetic (iEK) systems stimulated with direct current and low-frequency(< 1 kHz) AC electric fields. The article covers the surge of iDEP as a research field where many different device designs were developed, from microchannels with arrays of insulating posts to devices with curved walls and nano- and micropipettes. All of these systems allowed for the manipulation and separation of a wide array of particles, ranging from macromolecules to microorganisms, including clinical and biomedical applications. Recent experimental reports, supported by important theoretical studies in the field of physics and colloids, brought attention to the effects of electrophoresis of the second kind in these systems. These recent findings suggest that DEP is not the main force behind particle trapping, as it was believed for the last two decades. This new research suggests that particle trapping, under DC and low-frequency AC potentials, mainly results from a balance between electroosmotic and electrophoretic effects (linear and nonlinear); although DEP is present in these systems, it is not a dominant force. Considering these recent studies, it is proposed to rename this field from DC-iDEP to DC-iEK (and low-frequency AC-iDEP to low-frequency AC-iEK). Whereas much research is still needed, this is an exciting time in the field of microscale EK systems, as these new findings seem to explain the challenges with modeling particle migration and trapping in iEK devices, and provide perhaps a better understanding of the mechanisms behind particle trapping.

Keywords Dielectrophoresis · Electroosmosis · Electrophoresis · Electrokinetics · Microfluidics

Introduction

Microfluidics, a research field born in the 1990s owing to the advances in microfabrication techniques [1], has grown considerably during the last two decades. One of the main pillars of microfluidics is electrokinetics (EK), defined as the use of electric fields to manipulate particles and liquid in miniaturized systems [2]. An attractive feature of the subfield of microscale EK is that it exploits physical phenomena, i.e., no chemical reactions are required, making EK-based microsystems simpler than their chemical assay–based counterparts. Microfluidics has made a significant impact to the field of bioseparations; in particular, EK-based miniaturized devices have proved to be successful analytical platforms for many bioparticles of interest: DNA [3–5], proteins [6, 7], viruses [8–11], bacterial cells [10, 12–14], yeast cells [10, 15, 16], mammalian cells (including cancer and tumor cells) [17–20], and even parasites [21–23].

A main attribute of EK-based techniques is their ability to analyze bioparticles across multiple scales, from macromolecules to parasites. Macromolecules, which are ubiquitously electrically charged, have been successfully analyzed and manipulated with EK-based techniques for many decades [24, 25]. Applying EK-based techniques for the analysis, enrichment and purification of microorganisms are possible owing to the fact that all microorganisms possess electrical surface

ABC Highlights: authored by *Rising Stars and Top Experts.*

✉ Blanca H. Lapizco-Encinas
bhlbme@rit.edu

[1] Microscale Bioseparations Laboratory and Biomedical Engineering Department, Rochester Institute of Technology, Institute Hall (Bldg. 73), Room 3103, 160 Lomb Memorial Drive, Rochester, NY 14623-5604, USA

Published online: 19 October 2021

charges. Kłodzinska and Buszewski published an excellent article explaining the origins of microbial charge [26]. Briefly, electrical charges on the surface of microorganisms are the result of the ionization of surface molecules (proteins, lipids, teichoic acids, and lipopolysaccharides) and the adsorption of ions from the suspending electrolyte solution. Figure 1a illustrates a bacterial cell with a net negative surface charge and the cloud of ions, known as the electrical double layer (EDL), surrounding the cell; also included in the figure is the representation of the interactions between the negatively charged bacterial cell and a negatively charged surface of a fused-silica capillary used for capillary electrophoresis (CE) separations and analysis [26]. Understanding the origin and behavior of the electrical charge of microorganisms is essential for the design of engineered systems for the analysis, identification, and separation of microbes. Usually, the electrical charge of microorganisms is measured and reported as their zeta potential, as surface electrical charge cannot be measured directly; thus, EK measurements must be employed. Polaczyk et al. [27] recently reported the calculation of the zeta potential

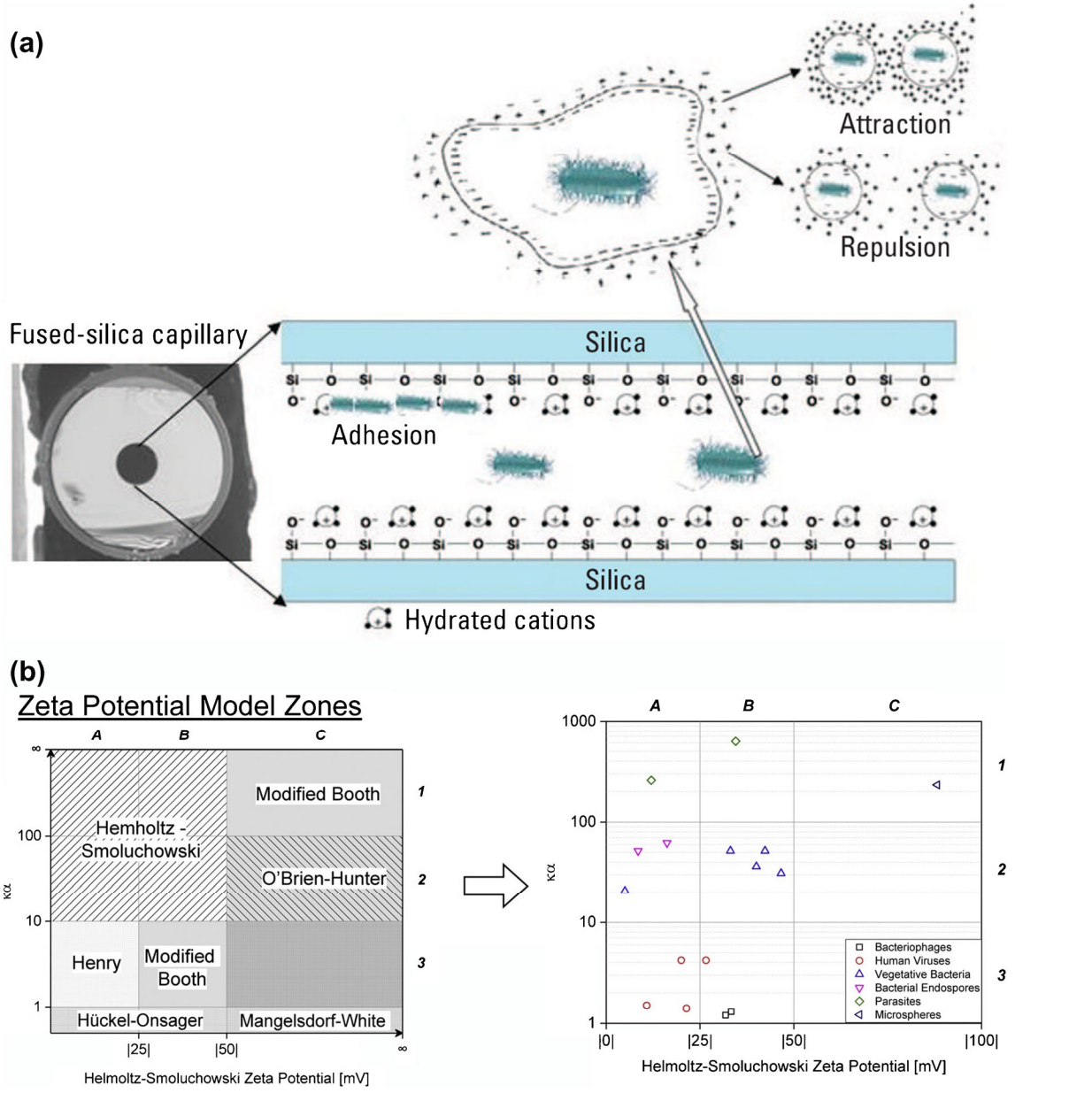

Fig. 1 **a**Representation of the charged surface of a bacterial cell depicting the cloud of ions surrounding the cell, and the interactions of the charged cell surface and a fused-silica capillary, adapted from [26], copyright (2009), American Chemical Society. **b** Chart summarizing the correlation of zeta potential models with microorganism type. The *y*-axis of the chart is the parameter $\kappa\alpha$, where κ is the reciprocal of the Debye length (λ) and α is the particle radius (for the rest of this article, a will be used to identify the particle radius). The chart is divided into nine regions, labeled A to C and 1 to 3. Adapted from [27], copyright (2020) Elsevier Ltd.

of several microorganisms from electrophoretic mobility assessments. This excellent study tested the applicability of the main theoretical models for zeta potentials to each type of microorganism: viruses, vegetative bacteria, bacterial endospores, and protozoa. Figure 1b illustrates a chart summarizing these findings that correlate zeta potential models with the type of microorganism. Polaczyk et al. [27] identified, for example, that the equation from the Helmholtz-Smoluchowski model was the most appropriate for bacterial cells, bacterial endospores, and parasites, while the modified Booth and Henry models were more appropriate for viruses.

The need for rapid and effective techniques for the detection of pathogenic microorganisms [28] has been one of the main driving forces of the rapid growth of microscale EK systems, as antibiotic-resistant bacteria [12] are a major threat to human health. Furthermore, the increasing demand for rapid diagnostic techniques for clinical applications in the detection of rare cells from peripheral blood has also pushed forward the growth and development of EK-based microsystems. Numerous reports have illustrated the use of EK techniques for the analysis of cancer and tumor cells, blood cells, stem cells, extracellular vesicles, and cell organelles [29]. The advances in EK-based methods have allowed highly sophisticated clinical assessments, such as the analysis of the stages of the malignancy of cancer cells [30–33] and characterization of T lymphocytes (T cells) [18, 34–36].

The present review article is focused on a specific sub-field of microscale EK devices: insulator-based dielectrophoresis (iDEP) systems, in particular systems stimulated with direct current (DC) and low-frequency(< 1 kHz) alternating current (AC) potentials [37, 38]. In these systems, the nonlinear EK effect is generated in precise regions within the devices, where the electric field magnitude is higher due to the presence of 3-dimensional electrical insulating structures [38, 39]. There is a plethora of iDEP designs that have been successfully employed that feature insulating posts, curved channel walls, sawtooth channel walls, etc. The section titled "First reports of insulator-based electrokinetic (iEK) microsystems" describes the pioneer research studies that started this rapidly growing research sub-field. The present review is proposing renaming the field of iDEP to insulator-based EK (iEK) systems. The justification for this proposal is that the more general term of iEK provides a more accurate description of the several EK phenomena that are present in these systems. The manipulation of particles and microorganisms in insulator-based EK systems is possible due to the effects of several phenomena, not only DEP. Particle trapping, for example, is the result of an equilibrium between the distinct forces acting on the particles that renders particles with a net electromigration velocity of zero. If an equilibrium is achieved in a given system, this means that several forces or phenomena are significant in that system. Thus, the name change for this field from iDEP to iEK provides a better description of the several EK phenomena behind particle manipulation and trapping in insulator-based systems.

This review article, with 180 references, describes the evolution of the field of iDEP microsystems under DC and low-frequency(< 1 kHz) AC fields. The introduction discusses the applicability of microscale EK systems in bioanalysis, which takes the advantages of both charge-dependent EK phenomena and charge-independent EK phenomena. The theory section presents a theoretical background outlining the main equations that describe the physics behind particle migration and trapping in these systems. The section titled "First reports of insulator-based electrokinetic (iEK) microsystems" illustrates how the field of insulator-based DEP (iDEP) was established. The cited reports in the following three sections of this article depict the progress and latest developments in this field. In particular, a discussion is included that describes how the term iDEP was coined and how an entire research sub-field was created around this term, specifically for systems stimulated with DC and low-frequency(< 1 kHz) AC potentials. A discussion on the recent reports on the effect of electrophoresis of the second kind in DC-iEK systems is included, which illustrates that DEP is not the main EK mechanism responsible for particle trapping, as trapping is a balance between two or more phenomena, and explains the surge of the new field of DC-iEK. The conclusions summarize the state of the art in this sub-field and speculate on the future developments.

Theory

The migration of particles in iEK systems is dictated by linear and nonlinear EK phenomena that act on the particles and on the fluid. Linear phenomena are defined as those that have a linear dependence with the electric field. In iEK systems, under the effects of DC and low-frequency(< 1 kHz) AC potentials, the main linear phenomena are electroosmotic (EO) flow and linear electrophoresis ($EP^{(1)}$), which can be grouped together as linear EK; the expressions for these three velocities are as follows:

$$\mathbf{v}_{EO} = \mu_{EO}\mathbf{E} = -\frac{\varepsilon_m \zeta_W}{\eta}\mathbf{E} \tag{1}$$

$$\mathbf{v}_{EP}^{(1)} = \mu_{EP}^{(1)}\mathbf{E} = \frac{\varepsilon_m \zeta_P}{\eta}\mathbf{E} \tag{2}$$

$$\mathbf{v}_{EK} = \mu_{EK}\mathbf{E} = \frac{\left(\mu_{EO} + \mu_{EP}^{(1)}\right)}{\eta}\mathbf{E} \tag{3}$$

where $\mathbf{v}$ represents the velocity, μ represents mobility, ε_m is the absolute electric permittivity of the fluid suspending medium, ζ is the wall zeta potential or the particle zeta potential, η is the viscosity of the suspending medium, and $\mathbf{E}$ is the electric

field. Equation (2) for the linear EP velocity follows the Helmholtz-Smoluchowski model, which is valid when the EDL is considered "thin" in comparison to the size of the particle ($\kappa a > > 1$), where κ is the reciprocal of the Debye length (λ) and a is the particle radius. Under different conditions, other models must be applied, such as the Hückel-Onsager model for small particles, etc. An excellent summary of the distinct models employed to relate $\mu_{EP}^{(1)}$ to ζ_P is included in Fig. 1b and described in detail by Polaczyk et al. [27].

Nonlinear EK phenomena are those that have a nonlinear dependence with the electric field. These phenomena arise when under the effects of an electric field, the diffuse layer of the EDL is deformed due to the formation of ion concentration gradients also known as concentration polarization. Briefly, when an electric field is present, the diffuse layer of the EDL around a charged particle is distorted; i.e., the screening of the particle surface charge is no longer uniform; in some regions of the diffuse layer, there is underscreening and in some regions there is overscreening [39]. Concentration polarization is the result of the flux of ions caused by the effects of the electric field, which, as described, alters the spatial distribution of the ions in the diffuse layer of EDL, deviating the diffuse layer from equilibrium, giving rise to nonlinear EK phenomena [40].

For the purpose of this review article, two nonlinear EK phenomena are considered under conditions of DC and low-frequency(< 1 kHz) AC electric fields: EP of the second kind and dielectrophoresis (DEP). When EP or EO velocities are one or two orders of magnitude greater than those predicted by Smoluchowky's theory, these phenomena are referred to as "second kind" phenomena [41]. An important concept to add here, related to concentration polarization, is the difference between the "first-kind" and the "second-kind" EK phenomena. The first kind or linear phenomena depend on the permanent surface charge, while the second-kind phenomena depend on the bulk charge, which is the result of concentration polarization. Furthermore, under certain conditions, second-kind EK phenomena can be up to two orders of magnitude greater than the first-kind phenomena [42]. There are several models that describe particle migration under the effects of EP of the second kind, since nonlinear electrophoretic phenomena can be categorized by two dimensionless parameters: the Dukhin number (Du) and the Peclet number (Pe) [43]. The Dukhin number (Eq. 4) is defined as the ratio of the surface conductivity (K^{σ}) of a particle to the bulk conductivity of the medium (K_m) times particle radius (a); thus, it is the competition between surface and bulk conductivity. At very small Du values, the deviation from linear EK behavior is not noticeable; however at $Du > > 0.1$, nonlinear EK effects are significant and must be considered [43]. In EK phenomena, the Peclet number (Eq. 5) describes the ratio of the convective transport to the diffusive transport of the electrolyte ions near the particle surface; thus, it is the competition between convection and diffusion of the electrolyte ions [40]. The particle radius (a) is used as the characteristic length in this expression (Eq. 5) to account for the thickness of the EDL and the thickness of the diffusion layer relative to the particle size [40, 42]. The Peclet number has a strong influence on the concentration polarization of the fluid surrounding a particle and on the EP velocity of a particle.

$$Du = \frac{K^{\sigma}}{K_m a} \tag{4}$$

$$Pe = \frac{av}{D} \tag{5}$$

where v is the magnitude of the particle EP velocity and D is the diffusion coefficient. The expression of the Peclet in number in EK depends on the magnitude of the electric field (as it depends on EP velocity) and particle radius [42]. There are numerous reports from the field of physics and colloids that describe EP of the second kind; of particular importance are the contributions by Dukhin [42, 44, 45], Mishchuk [46, 47], Shilov [48], Schnitzer and Yariv [49–51], Khair [52], and Barany [53]. The reader is referred to these references for further details on the theory of EP of the second kind. In the classical EP theory, the EP mobility of a particle with a thin EDL is constant, i.e., linear dependence with $\mathbf{E}$. For cases that deviate from the linear dependence, at low Pe numbers, the nonlinear EP velocity is proportional to the cubed strength of the electric field (E^3), while at large Pe numbers, with weak concentration polarization, the nonlinear EP velocity is proportional to $E^{3/2}$. For the case of large Pe numbers and strong concentration polarization, the complexity of the phenomena does not allow identifying a clear relationship. Recent studies [43, 54–56] that include experimental results have demonstrated that the linear dependence of the EP velocity (Eq. 2, $v_{EP} \sim E^{\mathbf{1}}$), is valid for $Pe \leq 1$ with $Du < < 0.1$, with weak concentration polarization. These reports [43, 54–56] also demonstrated the nonlinear dependences of the EP velocity with $\mathbf{E}$; the expressions for these velocities are [43]:

$$\mathbf{v}_{EP}^{(3)} = \mu_{EP}^{(3)}\mathbf{E^3} \text{ for } Pe << 1, Du > > 0.1, \text{with weak concentration polarization} \tag{6}$$

$$\mathbf{v}_{EP}^{(3/2)} = \mu_{EP}^{(3/2)}\mathbf{E^{3/2}} \text{ for } Pe > > 1 \text{ with weak concentration polarization} \tag{7}$$

It is essential to note that, since the value of Pe depends on the electric field ($\mathbf{E}$) and particle radius, it is possible for a small particle to satisfy the condition of $Pe < < 1$, and for a large particle to satisfy the condition of $Pe > > 1$, irrespective of the magnitude of the local electric field [40]. Mathematical complexities only allowed for the theory of nonlinear EP to be developed for the limiting cases of the value of Pe; i.e., theoretical models exist for low ($Pe < 1$) and high ($Pe > > 1$) values of Pe, but no theory has been developed for

intermediate values ($1 < Pe < 10$) [43]. An excellent summary discussing the theoretical models for nonlinear EP, showing the effect of the magnitude of both *Pe* and *Du* numbers, has been reported by Rouhi and Diez (see Table 1 in ref. [43]). For the specific case when *Pe* is less than or close to 1 ($Pe \leq 1$), the EP velocity has a linear dependence with electric field (as described by Smoluchowski's theory), if $Du << 0.1$, since at small values of the Dukhin number, the deviations from linear behavior are not appreciable [43].

Our group has investigated experimentally the effects of EP of the second kind in polystyrene particles, viruses, bacteria, and protein nanoparticles, where a dependence with $\mathbf{E}^3$ was observed [14, 55–58]. For further information and discussion on EP of the second kind in DC-iEK systems, the reader is also referred to an excellent review article by Perez-Gonzalez [39].

Another nonlinear EK phenomenon considered in this review is DEP, which is defined as particle migration under the effects of a nonuniform electric field due to polarization effects. In iEK devices, nonuniform electric field distributions are created by the presence of insulating structures, curved channel walls, etc. The expression for the DEP velocity for a spherical particle is defined as:

$$\mathbf{v}_{DEP} = \mu_{DEP}\nabla E^2 = \frac{a^2\varepsilon_m}{3\eta}\mathrm{Re}[f_{CM}]\nabla E^2 \tag{8}$$

where *a* is the particle radius and $\mathrm{Re}(f_{CM})$ is the real part of the Clausius-Mossotti factor, which accounts for the particle polarizability relative to that of the fluid-suspending medium. This expression is valid for a spherical particle with radius *a*, for which the Stokes drag force is $\mathbf{F} = 6\pi\mathbf{v}\eta a$. Until recently, it was believed that DEP was a dominant phenomenon in iEK systems under the effects of DC and low-frequency(< 1 kHz) AC potentials; the present review includes a discussion on this topic in the section titled "The missing link: electrophoresis of the second kind." The effects of nonlinear induced charge electroosmosis (also known as electroosmosis of the second kind) and nonlinear electrothermal flows are out of the scope of this review focused on highlighting the importance of electrophoresis of the second kind in insulator-based systems; therefore, these phenomena are not being discussed here. For a detailed discussion on these nonlinear EK phenomena, which can become significant when insulating structures with sharp edges are employed, the reader is referred to an excellent recent review article by Xuan [59] and the studies by the Buie research group [60].

First reports of insulator-based electrokinetic (iEK) microsystems

After the discovery of DEP by Pohl in the early 1950s [61], and subsequent reports by Pohl and collaborators that highlighted the use of nonhomogeneous electric field distribution for enhancing nonlinear EK effects [62–68], a strong interest on developing miniaturized devices that could produce nonhomogeneous electric fields was born. In particular, researchers were interested in exploiting DEP employing high-frequency AC electric fields, and many electrode-based DEP (eDEP) microsystems were successfully developed; several excellent reviews describe these pioneer studies on eDEP [69–71]. The focus of the present review is on iEK systems, in which nonhomogeneous electric field distributions are created by employing electrically insulating structures between electrodes. The first report on iEK was published by Masuda et al. [72] in 1989. They created a microdevice for cell fusion that employed EK effects. Briefly, they built a microfluidic device connected to two cell suspension reservoirs; each reservoir contained one type of cell, referred to as cell A and cell B, as depicted in Fig. 2a. By employing micropumps, they sent one cell of each type to a small opening between two insulating structures located between two electrodes. By energizing the electrodes, the two cells formed a pearl chain at the constriction due to positive DEP forces; then a pulse voltage produced a reversible break in the cells' membranes (by rupturing the phospholipid layer) forming a fused hybrid cell. The device by Masuda et al. demonstrated the first application of EK forces for the trapping of the cells at a specific location within an iEK device, which allowed for highly selective cell fusion. A similar device for EK-based cell fusion was recently reported by Gel et al. [73].

The second major advancement in the field of iEK devices was the work by Cummings and collaborators in 2000–2003 [74–77] at Sandia National Laboratories, with the design of simple glass microfluidic channels, which featured, for the first time, square arrays of 3D insulating posts of different shapes (cylindrical, square and diamond). A representation of these devices is included in Fig. 2b [78], this device had 12 independent channel regions, and each channel region contained six channels straddled by two liquid reservoirs. By employing these engineered systems stimulated with DC electric fields, Cummings et al. identified the regimes of particle "streaming" and particle "trapping" with 200-nm polystyrene particles [76, 77]; experimental images of these two particle migration regimes are depicted in Fig. 2c. In three follow-up studies, the Sandia research group demonstrated the differentiation between live and dead bacterial cells [78], the separation of distinct types of live bacterial cells [79], and the enrichment of tobacco mosaic virus [80]. The term insulator-based DEP (iDEP) was first coined in these two well-known studies [78, 79], and it has been significantly employed for almost two decades. Analogously, the term electrode-based dielectrophoresis (eDEP) [81] was also coined to describe the more traditional microfluidic devices that featured arrays of

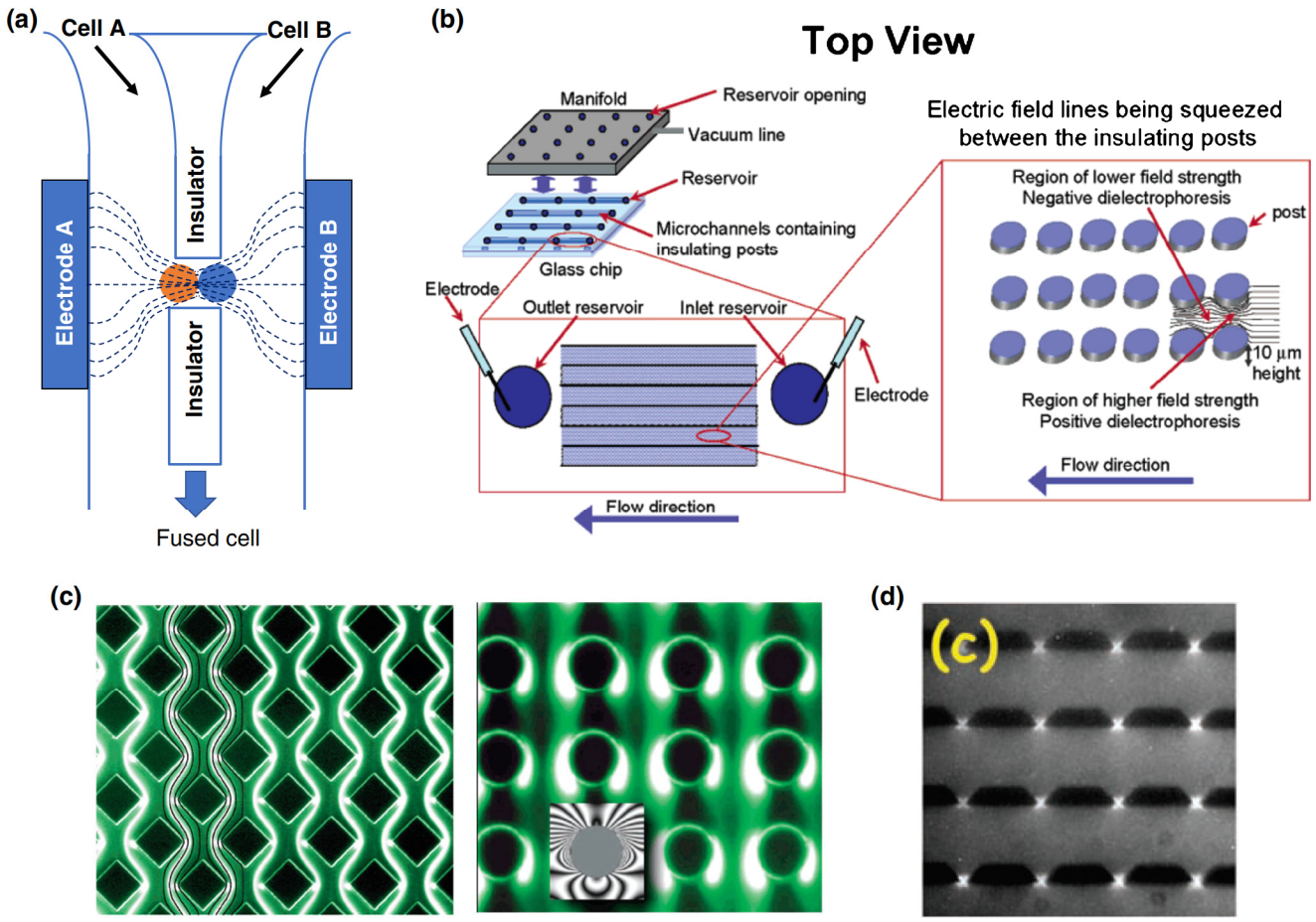

Fig. 2 **a** Representation of the device employed by Masuda et al. [72] for the fusion of two cells. One cell of each type is first sent at the constriction between the two insulating structures. By action of positive DEP, the two cells are trapped at the constriction forming a pearl chain, when a pulse voltage is applied that fuses the two cells together. **b** Representation of the iEK devices employed by Cummings et al. Reprinted with permission from [78], copyright (2004) American Chemical Society. **c** Images depicting particle streaming in a device with diamond-shaped posts and particle trapping in a device with cylindrical posts (the inset in grayscale depicts modeling results obtained in the same study); in both images, flow direction is from top to bottom. Reprinted with permission from [76], copyright (2003) American Chemical Society. **d** Image depicting the trapping of 368-bp dsDNA between trapezoid-shaped insulating posts made from glass; flow direction is from top to bottom. Adapted with permission from [82], copyright (2002) Elsevier

microelectrodes (usually planar) to generate the nonhomogeneous electric fields required to generate DEP effects.

Almost at the same time of the Sandia work, a similar device with uniformly arranged trapezoid-shaped insulating posts was reported by Chou et al. in 2002 [82] for the trapping of single-stranded and double-stranded DNA employing an AC electric potential of 5 V with low frequencies (< 1 kHz). Figure 2d illustrates enriched DNA molecules (shown bright white) trapped at the constriction between the posts. In a follow-up study [83], which featured devices with triangular-shaped insulating structures made from polydimethylsiloxane (PDMS), this group demonstrated cell sorting of bacterial cells, cell lysis of red blood cells (RBCs), and DNA purification and concentration. The publications by Chou et al. [82, 83] coined the term electrodeless DEP (EDEP); however, this term did not gain too much popularity as it could easily be mistaken for eDEP. The next section describes the major developments in the subfield of DC-iDEP systems, including a discussion of the many device designs featuring insulating posts, curved channel, etc.

The surge of direct current insulator–based dielectrophoresis (DC-iDEP)

The research at Sandia Laboratories [74–80] led the start of the subfield of DC-iDEP. Numerous devices featuring a variety of insulating structures or carefully designed curved channel walls were developed to generate nonhomogeneous electric field distributions as illustrated by recent review articles [37–39, 84, 85]. The next subsection presents a discussion on these device designs.

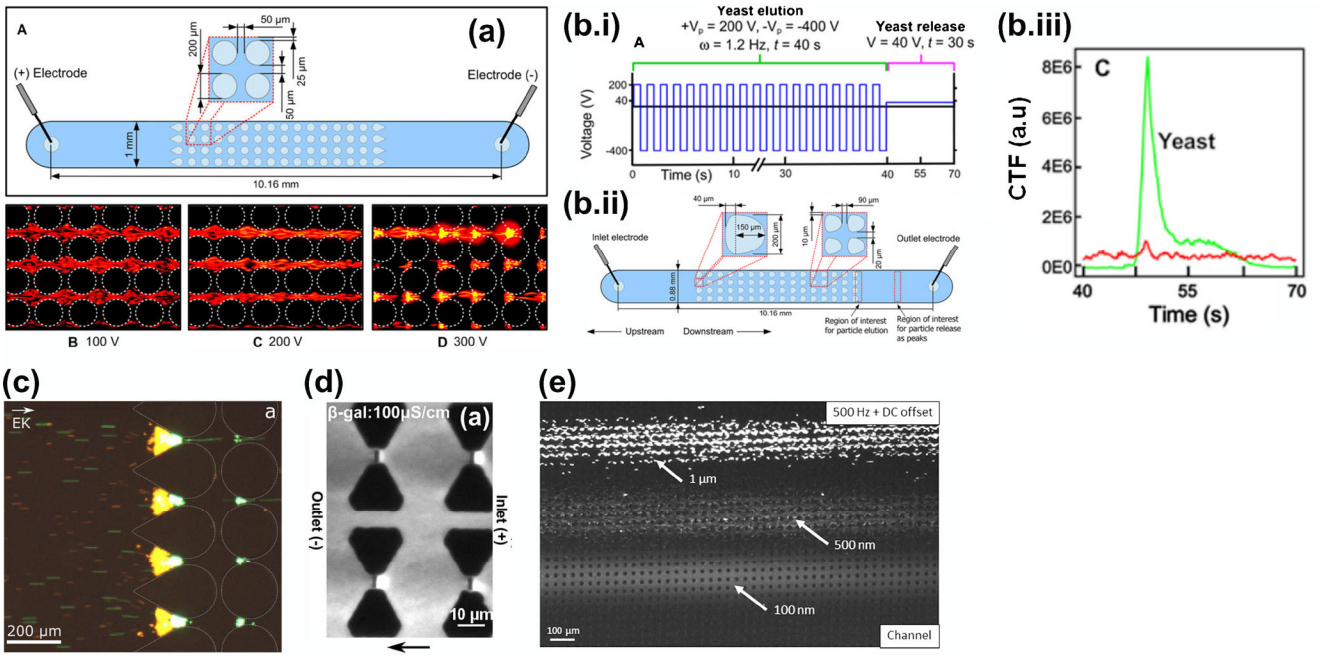

Fig. 3 **a** Representation of an iDEP device with cylindrical insulating posts and images of 1-mm red particles at three distinct applied potentials, illustrating particle streaming at 100 and 200 V and particle trapping at 300 V. Adapted with permission from [86], copyright (2015) John Wiley and Sons. **b**(i) Representation of the DC-biased step AC signal and (ii) top view of the iDEP device with asymmetric insulating posts used to separate yeast cells from 2-µm polystyrene particles, by eluting the yeast cell first. (iii) Graph of the "peak" of enriched yeast cells eluted from the system; cells were fluorescently labeled and the corrected total fluoresce was used for detection. Adapted with permission from [92], copyright (2016) John Wiley and Sons. **c** Trapping of gold-coated(orange) and plain (green) 2.4-µm polystyrene particles at 200 V_{DC}. Adapted with permission from [127], copyright 2019 AIP Publishing. **d** Trapping of β-galactosidase with micron-sized triangular posts and nano-sized rectangular posts. Adapted with permission from [108], copyright (2015) The Royal Society of Chemistry. **e** Separation of a mixture of three distinct sizes of polystyrene particles with DLD-iDEP. Reprinted from [113], copyright 2019 AIP Publishing

Devices with insulating posts

Microchannels with 3D insulating posts became popular as a result of the work at Sandia Laboratories [74–80]. A representation of an iDEP microchannel with cylindrical insulating posts is included in Fig. 3a, including three images of 1-µm red polystyrene particles illustrating the regimes of particle streaming at 100 and 200 V_{DC}, and particle trapping at 300 V_{DC} [86]. One attractive feature of these devices is their simplicity in fabrication, as the entire device, including the insulating posts, can be made from a single substrate. The most common materials are glass [76], PDMS [86], Zeonor [87], and PMMA [88]. Extending the work at Sandia Laboratories, Lapizco-Encinas employed iDEP devices made from glass and PDMS to demonstrate for the first time the trapping of protein molecules [89] in DC-iDEP systems. This group also worked with DNA [81]; algal, bacterial, and yeast cells [90–93]; bacteriophages [8]; nano-sized particles [94, 95]; and polystyrene particles [91, 96]. A main focus of this group has been on improving the geometry of the insulating posts to enhance particle manipulation and trapping. Their findings have demonstrated that sharper and narrower post shapes enhance particle trapping [97, 98] and that reducing the number of columns of insulating posts decreases the required electric potential to achieve particle trapping [99]. The Lapizco-Encinas group has employed DC potentials and low-frequency(< 1 kHz) AC potentials. In particular, they have developed several schemes for applying low-frequency AC potentials, such as an EO flow gradient [93] and DC-biased AC potentials combined with asymmetric insulating posts [92], as well as cyclical potentials [100]. These schemes with low-frequency AC and cyclical potentials exploited differences in particle electromigration in the post array that resulted in effective particle separations. For example, the combination of an asymmetric AC signal (DC-biased AC potential) with asymmetric insulating posts allowed changing the "elution order"—i.e., larger particles were eluted first, which is essential when handling fragile eukaryotic cells. Figure 3b.i shows the asymmetric DC-biased AC step function signal used to enrich and separate yeast cells from 2-µm polystyrene particles in less than 70 s; Fig. 3b.ii illustrates the asymmetric post iDEP device; and Fig. 3b.iii contains a graph of the "peak" of the separated yeast cells [92]. Another important contributor to iDEP is the research group at Tecnologico de Monterrey, with their unique work with pegylated proteins [101] and exosomes [102].

The research group led by Thöming and Pesch at the University of Bremen also studied the impact of insulating post shape and post material on particle trapping [103, 104], and their findings, in agreement with the Lapizco-Encinas group [97, 98], also indicated that shaper and narrower posts are better for enhancing particle trapping. In a more recent study, they published the first report on iDEP of gold-coated polystyrene particles and designed strategies for dealing with particle agglomeration in iDEP systems by adjusting the pH and conductivity of the suspending media. Figure 3c shows the trapping of gold-coated(orange) and plain (green) 2.4-μm polystyrene particles at 200 V_{DC} in an iDEP device with cylindrical insulating posts. The Casals-Terré group also studied in detail how insulating post shape and arrangement could be manipulated to improve particle trapping in DC-iDEP systems [105]; they proposed the use of a new parameter called the trapping value (T), which is discussed later in this article.

The Ros group at Arizona State University has made major contributions to iDEP. They have demonstrated the manipulation of DNA [106], proteins [107, 108], carbon nanotubes [109], cell organelles [110], and cells [111, 112]. In 2015, this group proposed the unique combination of nano-sized and micron-sized insulating posts within the same device. Shown in Fig. 3d is an image of fluorescently labeled β-galactosidase molecules trapped at 50 V_{DC} employing micron-sized triangular posts and nano-sized rectangular posts located between the triangular posts. This strategic approach, which created nanometer-sized constriction between posts, significantly decreased the required DC electric potential to achieve trapping.

Another important trend in iDEP devices with insulating posts is combining deterministic lateral displacement (DLD) with DEP. The Morgan group has made several important contributions [113–115] where they employed DC-biased low-frequency AC potentials with devices with cylindrical insulating posts. In DLD, particles migrate in a continuous mode across a post array arranged at a specific angle (usually < 6°); by having the posts tilted, particles that are larger than the critical diameter (Dc) bump onto the post, and their migration is deviated by the tilt angle, while smaller particles continue flowing straight through in a zigzag pattern. This type of continuous particle migration is similar to the particle streaming regime identified by Cummings [77]. Figure 3e shows the separation by size of a mixture of 100-nm, 500-nm, and 1-μm polystyrene particles, illustrating a clear separation between the three particle populations by applying 320 Vpp at 500 Hz with a DC offset of − 0.25 V. As it can be seen, low-frequency AC DLD-iDEP devices require rather large post arrays (when compared with a "classic" iDEP channel, such as the one in Fig. 3a), which are wide enough for distinct particle populations to separate along the post array width. In this work by Calero et al. [113], the post array measured 2.6 mm by 31.2 mm.

Devices with insulating structures on the microchannel wall

A prominent trend developed in iDEP systems was the use of devices with insulating structures on the microchannel walls, creating devices with an array of single constrictions along the channel width. The Hayes group at Arizona State University has made the most contributions; they have worked with polystyrene microparticles, bacterial cells, viruses, RBCs, and even mammalian cells [116–124]. They called their designs gradient iDEP (g-iDEP), since the insulating sawtooth structures increased in size along the channel length, creating zones of gradually increasing electric field intensity.

One of their many significant contributions was the differentiation of three *Escherichia coli* serotypes by assessing the required average electric field to trap the particles (E_{app} = applied voltage/channel length). They also defined a threshold electric field (E_{onset}) which occurred when the applied electric potential was sufficient for particles to begin to accumulate and trap near the entrance of the constriction between two saw teeth. Figure 4a depicts a representation of a g-iDEP channel and a series of images of trapped *E. coli* cells at increasing voltages, illustrating that the number of trapped cells strongly depends on the applied voltage. The Hayes group has also made major contributions to the understanding of the forces behind particle trapping and has established the resolution theory [125] and determined an expression for the trapping condition of particles [126], which is discussed later in this article.

Another major contributor to iDEP is the Xuan group at Clemson University. In 2020, this group reported the passive DEP–based focusing of polystyrene particles (3, 5, and 10 μm) and yeast cells (5 μm) [128] employing micro channels with symmetrical and asymmetrical triangular insulating structures on the channel wall (similar to the device shown in Fig. 4b). Employing these devices, and under the effects of DC potentials, they achieved tight streams of highly focused particles and cells. The overall electric field in their systems were 250 V/cm and 312.5 V/cm for the polystyrene particles and cells, respectively, which should result in nonlinear EK effects at the constriction regions. Their work included mathematical modeling where a correction factor of 0.7 was employed to adjust for the DEP velocity. More recently, this group published an "infinite" microchannel, with triangular insulating structures on the channel wall (Fig. 4b), for the continuous focusing of the same types of polystyrene particles and yeast cells, but this time they used low frequency AC potentials [129]. They developed a clever strategy where particles, under the effects of the applied AC field, move back and forth inside the channel as EO and EP forces change direction with the AC field, while DEP forces remain unchanged (as DEP does not depend on field direction). This periodic process resulted in particles gradually being tightly

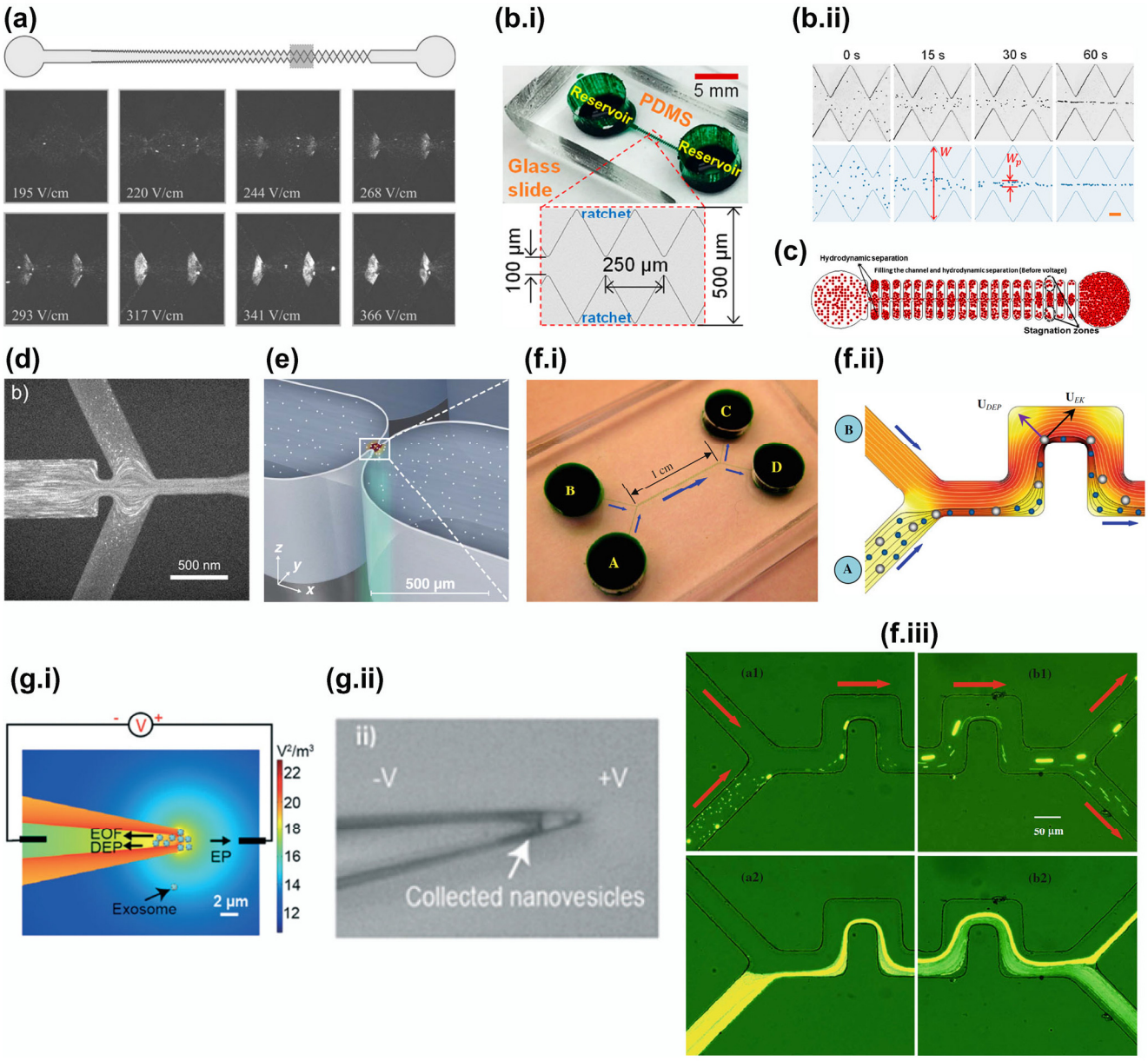

Fig. 4 **a** Representation of a g-iDEP channel and images of fluorescently labeled *E. coli* cells (strain O6:k1:H1) as function of the applied DC potential (reported as E_{app} in a 4.1-cm-long channel). Reprinted with permission from [167], copyright (2016) Springer Nature. **b** Image of the "infinite" channel with triangular insulating structures on the channel wall, and experimental and numerical results illustrating the gradual focusing of 5-µm polystyrene particles after a total time of 60 s, resulting in a tight stream of particles at the channel centerline. Adapted with permission from [129], copyright (2021) American Chemical Society. **c** Device with rounded insulating structures on the channel wall used for the separation of RBCs from plasma. Adapted with permission from [135], copyright (2015) Springer Nature. **d** Device with a single constriction used for the sorting of protein nanocrystals. Adapted with permission from [144], copyright (2015) American Chemical Society. **e** Illustration of a magnified view of the device with the 3D constriction used by the Bui group to study the relationship between extracellular electron transfer and surface polarizability of bacterial cells. Reproduced from [147], copyright (2019) Wang et al., open access article under the Creative Commons Attribution Non Commercial License 4.0 (CC BY-NC). **f**(i) Serpentine channel used for size-based separations. (ii) Depiction of the forcer generated at the corners of the channel walls. (iii) Four experimental images demonstrated effective size-based sorting of 5-µm and 1-µm particles under a resulting field of 15 kV/m; the left column and right column images are taken at the channel inlet and outlet, respectively. The top images are single snapshots while the bottom images are superimposed images. Adapted with permission from [160], copyright (2011) Springer Nature. **g**(i) Representation of the EK forces in the micropipettes, (ii) trapping of nanovesicles at the micropipette tip. Adapted with permission from [166], copyright (2019) The Royal Society of Chemistry

focused to the channel centerline, as depicted in Fig. 4b, after four 15-s periods (60 s total), all particles are efficiently focused to the channel centerline. This work also included mathematical modeling that required the use of correction factors. The Xuan group has also investigated the enrichment of nanoparticles by taking advantage of Joule heating effects

in these systems [130] and the focusing and trapping of particles in non-Newtonian fluids [131].

Another major contributor to this area is the Swami group at the University of Virginia; they have published extensively on the use of high-frequency AC potentials with iDEP and proposed the use of nano-constrictions [132, 133] (similar to the Ros group [108]). In their work with low-frequency AC fields, this group developed devices with triangular insulating structures on the channel walls for enhancing DNA hybridization. They called this strategy "constriction-based DEP," and demonstrated that DEP effects enhanced the transport of DNA molecules to the vicinity of a sensor, enabling pre-concentration, hybridization, and sensing without any wash steps. A unique characteristic of this work is that they were able to carry the entire process under conditions of high-conductivity suspending medium, which is highly challenging. Their work illustrated that enhancing sensing operations by means of iDEP allows decreasing the sensing limit down to 10 pM [134].

The Casals-Terré group, at the Technical University of Catalonia, also contributed to this area; they developed a device with distinctive curved insulating structures on the channel wall; this device is shown in Fig. 4c [135]. This system was successfully employed for separating RBCs from plasma under the action of DC fields and hydrodynamic effects. First, a sample of whole blood is introduced by capillarity into the channel, followed by the trapping of RBCs at the stagnation zones at the dead-end branches by hydrodynamic effects. The second step is when a DC voltage is applied, where negative DEP forces prevent the RBCs from entering the main channel, thus producing an RBC-free zone plasma zone within the main channel, as shown in Fig. 4c [135].

Devices with a single constriction

Another major approach developed in iDEP was devices with a single constriction and several outlets, which were used for continuous particle sorting. In these systems, a single insulating hurdle produced enough DEP effects that directed distinct particles to distinct outlets within the device, achieving effective particle sorting. The Li group was a pioneer in this area, developing several devices [136–138]; some of them even combined embedded electrodes with iDEP [139]. The Kirby group studied electrothermal flow effects in these systems, and their findings demonstrated that particle deflection and trapping are enhanced by the perturbations in the EO flow caused by electrothermal effects [140]. More recently, the Minerick group studied a DC-iDEP device for the sorting of polystyrene particles by size [141] and RBCs by ABO-Rh blood type [142]. Their results showed that DC-iDEP devices have potential for applications in rapid blood typing in clinical settings. Another major player in single-hurdle DC-iDEP systems is the Ros group at Arizona State University [143, 144]. They were the first group to report the sorting of protein nanocrystals with DC-iDEP systems. Figure 4d shows one of the devices used by the Ros group for the sorting by size of protein nanocrystals; in this device with three outlets, negative DEP forces exerted at the single-constriction region in the device deflected smaller crystal to the two side channel, while larger crystals were focused to the center outlet [144]. Their work illustrated that DC-iDEP devices can handle high-throughput operations with high efficiency (> 90%) that can be used for subsequent serial femtosecond crystallography experiments. This report demonstrated the suitable capabilities of these systems in protein crystallography. The authors speculated that this particular device could also be extended to DNA and carbon nanotubes sorting applications, thus showcasing the versatility of iDEP microfluidic sorters. The Xuan group at Clemson University also reported the use of single-constriction devices for the focusing of microparticles using DC-biased low-frequency AC potentials [145]. Another important trend initiated by the Xuan group is reservoir-based iDEP [146, 147], which mainly consisted of particle manipulation and trapping at the constriction between the large inlet liquid reservoir and the main channel. The Esfandiari group at the University of Cincinnati [148] also employed a single-constriction device with triangular insulating structures in their integrated lab-on-chip system for the enrichment and electrical impedance characterization of nanovesicles.

The Buie group at Massachusetts Institute of Technology [88, 149] also contributed to the development single-constriction systems with the creation of a 3D-iDEP device, where constrictions between the insulating structures were 3D, i.e., the constriction regions were also constricted along the height of the microchannel. This ingenious design worked similarly to the nano and micropost combination proposed by the Ros group [108]; the reduced constriction resulted in lower voltages required to achieve particle or cell trapping. Figure 4e illustrates a magnified view of the device with the 3D constriction that this group recently employed to study the relationship between extracellular electron transfer and surface polarizability of bacterial cells [150]. An alternative novel application of iDEP systems was proposed by the Yang group in 2019 [151] by developing devices for cell electroporation. They took advantage of the characteristic of these devices to generate zones of higher electric field intensity, by using these zones as electroporation zones. A follow-up study was recently published [152]; this study, which considers EP of the second kind, is discussed in the section dedicated to DC-iEK systems.

Devices with curved channel walls

Besides using insulating structures, non-homogeneous electric field distribution in a microfluidic device can be created with curved channel walls. The Xuan group at Clemson

University has made the most contributions to this subfield [153–160]. Their first reports in 2009 [153–155] illustrated the efficacy of these devices for rapid, label-free, and continuous particle sorting by taking advantage of the electric field distortion formed by the curvature of the channel walls. One of the devices used by the Xuan group is shown in Fig. 4f.i. This serpentine device with two inlets and two outlets was successfully employed for separating microparticles and cells by size [160]. As it can be observed from Fig. 4f.ii, DEP forces are generated at the corners of the channel wall, where negative DEP will deflect larger particles towards the channel centerline in a stronger manner than smaller particles; this is how size-based separation is achieved in this ingenious system. The four images in Fig. 4f.iii show the particles at the inlet and outlet of the channel under an effective field of 15 kV/m. At the channel inlet, it is observed that the particle suspension, containing randomly distributed 1-μm and 5-μm particles, enters from the bottom inlet reservoir, while at the outlet, the sorted particles exit the channel as two distinct particle populations directed towards distinct reservoirs, thus illustrating a complete separation. Similar excellent results were achieved for the separation of yeast cells from 3-μm particles, with a sorting efficiency > 90%. Furthermore, this device was proven to be successful with an estimated high throughput of 200 particles or cells per minute and can operate in a continuous manner for 15 min. The authors discussed the potential of this DC-iDEP serpentine device in biomedical and clinical applications. A device that combined insulating obstacles and curved walls (S-shaped channel) was proposed by Li et al. in 2013 [161] for the size-based separation of larger (10-μm and 15-μm diameter) polystyrene particles. The authors discussed that the combination of insulating obstacles with curved walls proved a greater control of particle migration.

Devices featuring nano- and micro-pipettes

Another form or DC-iDEP systems are nano- and micropipettes. The conical shape of the pipette provides a decreasing cross-section area that creates a nonhomogeneous electric field distribution along the pipette length, enhancing nonlinear EK effects. Some of the first reports were the nanopipettes developed by the Klenerman group for the manipulation of DNA and proteins [162–164]. This group demonstrated biomolecule enrichment and characterization by assessing surface conductivity. More recently, the Esfandiari group at the University of Cincinnati [165, 166] used nano- and micropipettes for the rapid enrichment of nanoparticles, liposomes, and extracellular vesicles (EVs) from bodily fluids. This group developed a narrow 1-μm-diameter tip pipette to extract EVs from plasma [165] and a four-parallel pipette system [166] which was used with plasma and saliva samples. The parallel system allowed processing larger sample volumes (200 μL total, 50 μL per pipette). The pipettes were made from borosilicate glass and had pore diameters of 1 and 2 μm. Figure 4g.i shows a schematic representation of the EK forces present in one pipette, while Fig. 4g.ii contains an image of trapped nanovesicles from human plasma at a DC field of 10 V/cm applied for 10 min. This system is an excellent example of the potential of EK devices in clinical and biomedical applications.

Devices featuring glass beads, nano- and microporous membranes

There is substantial flexibility on how insulating structures can be used in microfluidics devices to generate nonhomogeneous electric fields, which in turn enhance nonlinear EK effects. The field of DC-iDEP and low-frequency AC-iDEP systems also includes devices that feature microporous membranes made from an insulating material and, thus, effectively distort the electric field distribution. These types of membrane-based iDEP systems have been used to manipulate cells and microparticles [168, 169]. Glass beads, contained in a chamber straddled by two electrodes, have also been used to create nonhomogeneous electric fields, allowing for the use of nonlinear EK effects for the filtration and recovery of microbes from water [170, 171].

The missing link: electrophoresis of the second kind

During the surge of the field of DC-iDEP and low-frequency AC-iDEP, many mathematical models were also developed to predict the performance of EK devices as they were continuously gaining more attention. One of the first models was the potential flow solver “Laplace” developed by Cummings and Singh [76], which solved a modified Laplace equation. Other models, also based on the Laplace equation, were developed later on to predict the “trapping condition” illustrated in Eq. (9), to define the location of the particle-trapping region within the insulating post array. Figure 5a illustrates the results by the Lapizco-Encinas group on predicting particle trapping in a device with cylindrical posts; the top image is the model prediction and the bottom image is the experimental result [172]. It is important to note that correction factors, added to the model, were necessary for the model to agree with experimental results [173, 174], as illustrated by the parameter c added to Eq. (9). In a more recent study, this group defined the term “trapping barrier” and was able to predict the location of a “barrier” that the particles could not penetrate, resulting in a band of trapped particles as shown in Fig. 5b. This image is a superposition of modeling results and experimental results, where a correction factor of $c = 43$ was added to the model. Significant research efforts were devoted by numerous groups

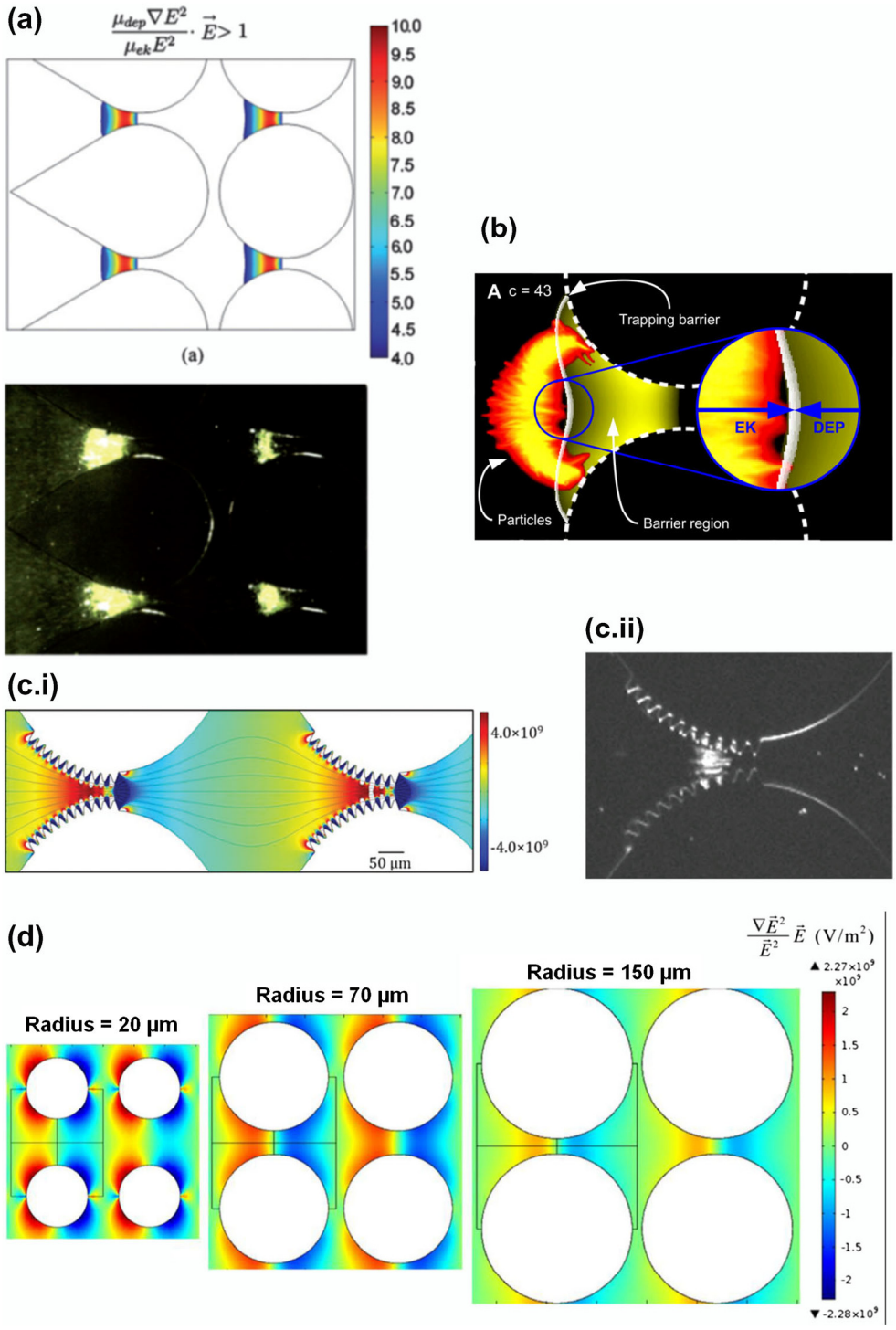

Fig. 5 **a** Prediction of the particle-trapping region with COMSOL (top) and experimental results (bottom) under the same conditions for 1-µm particles trapped in a device with 470-µm-diameter cylindrical insulating posts with 40-µm gaps. Adapted with permission from [172], copyright (2009) The Royal Society of Chemistry. **b** Prediction of the trapping "barrier" for 2-µm particles in a device with circular posts (200-µm diameter) and 50-µm gaps. The image is a superposition of modeling and experimental results. The barrier region was obtained with modeling with a correction factor of $c = 43$, while the band of trapped particles was obtained experimentally. Adapted with permission from [86], copyright (2015) John Wiley and Sons. **c**(i) illustration of the distribution of $\frac{\nabla|\mathbf{E}|^2}{\mathbf{E}^2}\cdot\mathbf{E}$ in the multi-scale device (circular posts with triangular nano-teeth) used by the Hayes group. (ii) Trapping of 2.7-µm silica particles at 600 V_{DC}. Adapted with permission from [126], copyright (2017) The Royal Society of Chemistry. **d** Prediction of the parameter $\frac{\nabla\mathbf{E}^2}{\mathbf{E}^2}\mathbf{E}$ in devices with circular insulating posts of three distinct sizes, with longitudinal and transversal distances of 20 µm and 30 µm, respectively. Adapted with permission from [105], copyright (2016) Springer Nature

to identify correction factors in DC-iDEP systems as reported by this recent review article [175]. As it is discussed below, it is possible that the need for correction factors was the result of not considering the effects of EP of the second kind. An excellent discussion on this was recently published by Perez-Gonzalez [39].

$$c\frac{\mu_{DEP}\nabla\mathrm{E}^2}{\mu_{EK}\mathrm{E}^2}\cdot\mathbf{E}>1 \tag{9}$$

The Kwon [176] group also developed a mathematical model to predict the trapping condition using Eq. (9); their

model optimized microchannel geometry. The Hayes group published in 2011 the experimental characterization of DEP mobility [117], where they noted that experimentally measured values of μ_{DEP} were lower than what would be necessary to achieve particle trapping. In a more recent report from 2017, the Hayes group defined dielectrophoretic trapping with the expression shown in Eq. (10) [126], which they evaluated with COMSOL in devices with different shapes of insulating posts (they tested 40 shapes), including devices with multi-scale insulators (circular post with triangular nano-teeth).

$$\frac{\nabla|\mathbf{E}|^2}{\mathrm{E}^2}\cdot\mathbf{E}\geq\frac{\mu_{EK}}{\mu_{DEP}} \tag{10}$$

Figure 5c.i illustrates the distribution of the parameter $\frac{\nabla|\mathbf{E}|^2}{\mathrm{E}^2}\cdot\mathbf{E}$ in the multi-scale device used by the Hayes group as predicted with COMSOL, and Fig. 5c.ii shows the experimental trapping of 2.7-μm silica particles at an applied voltage of 600 V_{DC}. This work illustrated that using the multi-scale designs resulted in a more homogeneous electric field distribution, eliminating extraneous particle trapping. Another major contribution by the Hayes group was identifying the parameter $\frac{\mu_{EK}}{\mu_{DEP}}$ (RHS in Eq. 10), as the electrokinetic mobility ratio (EKMr = $\frac{\mu_{EK}}{\mu_{DEP}}$); this parameter was used as electrokinetic signature to identify subtle differences in the electrokinetic response between cells and microparticles [123, 124]. The Hayes group also studied how dielectrophoretic data obtained in g-iDEP systems could be used to predict cell properties; for these assessments, they measured the fluorescence signal of trapped cells and studied how fluorescence intensity varied with the applied DC potential.

The Casals-Terré group also made major contributions to the prediction of the conditions under which particle trapping occurred in iDEP systems [105]. They studied how the spacing (longitudinal and transversal distance) between insulating posts and post radius affected particle trapping, and proposed the use of a new parameter, called the trapping value, which was defined as

$$T\equiv\frac{\nabla\mathbf{E}^2}{\mathbf{E}^2}\mathbf{E} \tag{11}$$

In their study, they evaluated in detail the effect of post spacing and post size on particle trapping in terms of the trapping value. They performed extensive modeling with COMSOL and experimentation. Figure 5d shows an example of their modeling results by illustrating the distribution of $\frac{\nabla\mathbf{E}^2}{\mathbf{E}^2}\mathbf{E}$ for insulating posts of three distinct sizes. As it can be observed, from the color scale in the figure, higher magnates of $\frac{\nabla\mathbf{E}^2}{\mathbf{E}^2}\mathbf{E}$ are reached with the smaller insulating posts (20-μm radius). The average value of T was 7.38 × 10^8, 6.63 × 10^8, and 3.60 × 10^8 V/m^2 for the three post sizes, respectively [105].

All of these models for trapping condition, mobility ratio (EK Mr), and trapping value (T) were excellent contributions that advanced the understanding of the force balance behind EK particle trapping in iEK devices. However, as illustrated by the Hayes group in 2011 [117], experimental measurements of DEP forces were lower than what was required to achieve particle trapping. None of the models proposed seemed to fully explain this discrepancy. That is why the use of correction factors added to mathematical models for iDEP systems gained popularity [175]. However, it is believed by the author of this review article that the reason why mathematical models were unable to accurately (without correction factors) predict particle trapping in these systems was because a major nonlinear EK phenomenon was not being included in these models. This missing phenomenon—or missing link—is EP of the second kind, which is briefly described in the "Theory" section of this review article. The importance of EP of the second kind has been described in many reports in the field of physics and colloids [42, 45–51], and an excellent discussion was recently published by Perez-Gonzalez [39]. Recent experimental work by Rouhi and Diez. [43] and Tottori et al. [54] studied the electrophoretic velocity of microparticles with particular focus on nonlinear EP effects. Rouhi and Diez studied ultrafast EK by applying a high electric field to microparticles of a variety of materials and compared their results with a wide range of data available in the literature [43]. In their report, they illustrated that EP velocity of the second kind, as explained in the "Theory" section in the present article, can have a dependence with $\mathbf{E}^3$ or $\mathbf{E}^{3/2}$ depending on the experimental conditions (magnitude of *Pe*, *Du* and concentration polarization [43]). Figure 6a.i-a.ii contains experimental results that illustrate the dependences of $\mathbf{v}_{EP}$ with $\mathbf{E}^3$and $\mathbf{E}^{3/2}$, respectively, from the data that Rouhi and Diez analyzed from the literature [43]. In Fig. 6a.i, the data obtained by Mishchuk [47] (inverted triangles and diamonds) exhibit an excellent fit with the $\mathbf{E}^3$ dependence, while in Fig. 6a.ii, the experimental data by Kontush [177] (squares and triangles) is in great agreement with the $\mathbf{E}^{3/2}$ dependence. The work by Rouhi and Diez [43] unveiled that EP velocity depends greatly on the magnitude of the local field strength, and categorized this behavior into three groups. Tottori et al. [54] employed a simple microchannel made from PDMS to analyze the electromigration of submicron particles made from polystyrene and poly-(methyl methacrylate) (PMMA) under high electric fields. In their work, this group observed that at high electric fields the particles were not able to enter the channel, as the device had a constriction region at the channel entrance, as depicted in Fig. 6b.i. This constriction produced a region of higher electric field intensity where nonlinear EP effects became dominant preventing the particles from entering the channel, as their EP migration is towards the inlet for these negatively charged particles. Tottori and collaborators were the first to propose that the phenomenon of particle trapping

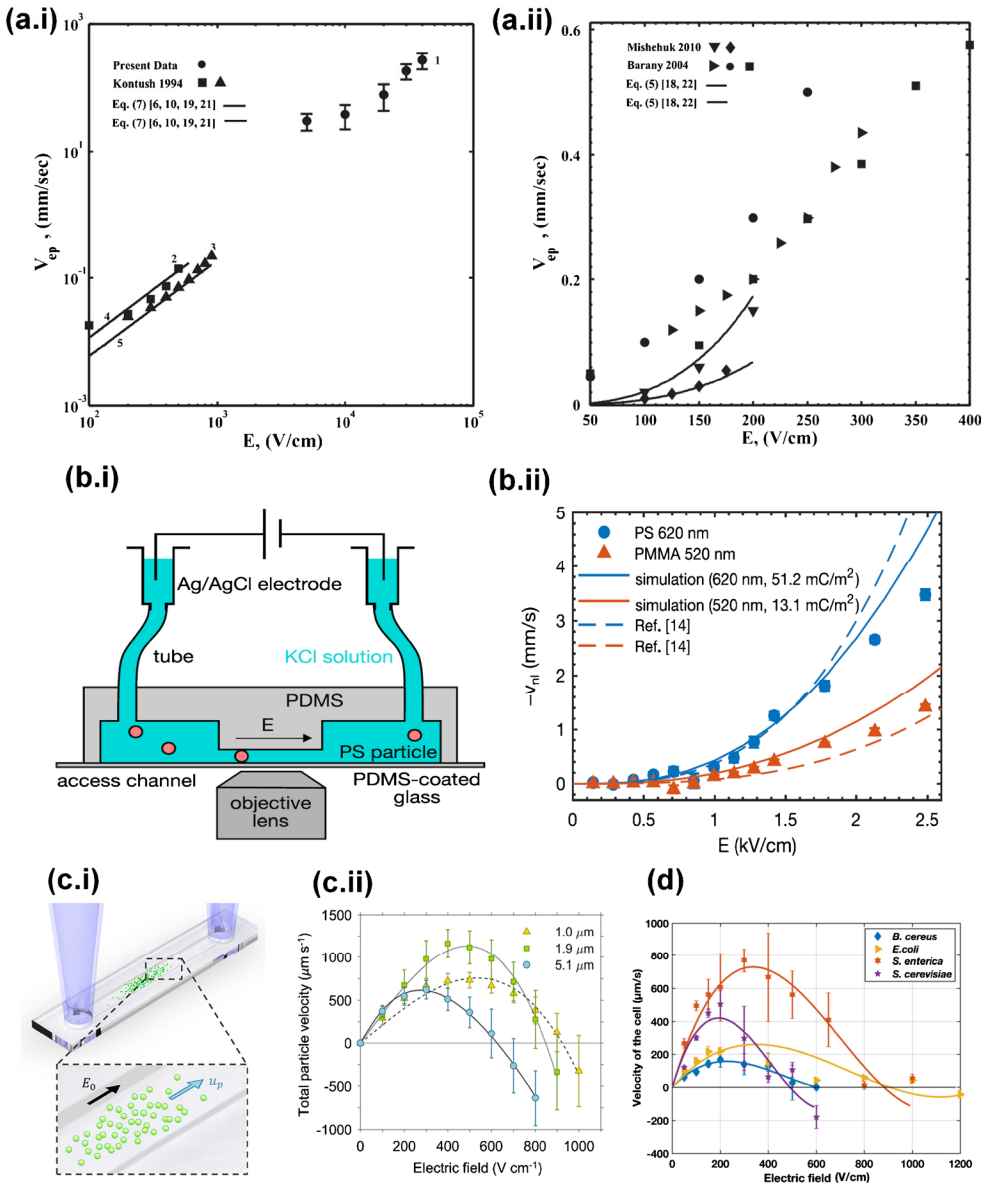

Fig. 6 Reports illustrating the importance of electrophoresis of the second kind. **a**(i) EP velocity as a function of the applied field illustrating the dependence with $\mathbf{E}^3$; see data by Mishchuk [47] (inverted triangles and diamonds). (ii) EP velocity as a function of the applied field illustrating the dependence with $\mathbf{E}^{3/2}$; see data by Kontush [177] (squares and triangles). Adapted from [43], copyright (2016) John Wiley and Sons. **b**(i) Illustration of the device used by Tottori et al.; please note the constriction at the channel entrance. (ii) Nonlinear EP velocity (v_{ln}) as a function of the electric field. Adapted from [54], copyright 2019 American Physical Society. **c**(i) Microchannel used for velocity assessments by Cardenas-Benitez. (ii) Particle velocity as a function of the electric field. Adapted from [55], open access article under the Creative Commons Attribution (CC-BY-NC-ND) 4.0 license (2020). **d** Velocity of bacterial and yeast cells as a function of the electric field. Adapted from [56], copyright (2020), American Chemical Society

observed in their system was not due to DEP (as it had been believed for the so-called DC-iDEP systems); they explained that particle trapping, which was a function of the electric field, was better explained by nonlinear EP effects. Their experiments included high-speed video tracking that allowed them to accurately extract particle mobility data and compare with mathematical modeling. Figure 6b.ii shows the dependence of the nonlinear EP velocity (v_{ln}) as a function of the electric field, where the dashed lines represent the EP velocity dependence with $\mathbf{E}^3$ (model by Schnitzer and Yariv [50]), and the solid lines are their own simulations with the Stokes-Poisson-Nernst-Planck(SPNP) model [54]. The recent work by Cardenas-Benitez [55] confirmed these findings by Tottori et al. [54]: the EK effect responsible for particle trapping in DC-iEK systems is not DEP, it is the balance between EP of the second kind, linear EP, and EO flow. Cardenas-Benitez [55] investigated the migration of negatively charged polystyrene microparticles in a plain (post-less) PDMS microchannel as illustrated in Fig. 6c.i. Since the channel used in this work did not have any type of constrictions or posts, there are no DEP effects present in the system. The total particle velocity was assessed under the action of DC potentials, and the particle behavior in Fig. 6c.ii was observed, where three distinct regimes can be identified: (i) linear velocity at low electric fields, (ii) a maxima velocity at medium-strength fields, and (iii) a decreasing velocity that even turns negative at higher fields. The authors concluded that EP of the second kind, which becomes significant at higher electric fields, is the phenomenon responsible for ending the linear increase in the total particle velocity and decreasing the velocity as the electric field increases. The effects of EP of the second kind are so strong that all particles reached a negative velocity (i.e., the

particle velocity was reversed, towards the inlet). Furthermore, under their experimental conditions, the authors also concluded that EP of the second kind had a dependence with $\mathbf{E}^3$ (as was also reported by Tottori et al. [54]). In a follow-up study, Antunez-Vela et al. [56] used the same system to characterize the migration of polystyrene microparticles and bacterial and yeast cells. Figure 6d shows the velocities of the yeast and bacterial cells as function of the electric field, where the same exact behavior can be observed: (i) linear increase, (ii) velocity reaches a maximum, (iii) followed by a velocity decrease (even reaching a negative velocities), confirming the findings of Tottori et al. [54] and Cardenas-Benitez et al. [55]. A major contribution proposed by Cardenas-Benitez [55] was the identification of the electrokinetic equilibrium condition (E_{EEC}), which is defined as the local electric field magnitude required to balance EO flow with linear and nonlinear EP migration, producing a net particle velocity of zero ($\mathbf{v}_P = 0$). Considering that in the microchannel used by Cardenas-Benitez the electric filed is uniform, as there were no insulating posts or any other structures that produce an electric field gradient, then no DEP forces were present; thus, for this system, the expressions for the total particle velocity (for $\mathbf{v}_P = 0$), E_{EEC} and $\mu_{EP}^{(3)}$, can be written as:

$$\mathbf{v}_P = \mathbf{v}_{EO} + \mathbf{v}_{EP}^{(1)} + \mathbf{v}_{EP}^{(3)} = \mu_{EO}\mathbf{E} + \mu_{EP}^{(1)}\mathbf{E} + \mu_{EP}^{(3)}\mathbf{E}^3 = 0 \quad (12)$$

$$E_{EEC} = \sqrt{-\frac{\left(\mu_{EP}^{(1)} + \mu_{EO}\right)}{\mu_{EP}^{(3)}}} \quad (13)$$

$$\mu_{EP}^{(3)} = -\frac{\left(\mu_{EP}^{(1)} + \mu_{EO}\right)}{{E_{EEC}}^2} \quad (14)$$

where $\mu_{EP}^{(3)}$ and $\mathbf{v}_{EP}^{(3)}$ are the nonlinear EP of the second kind mobility and velocity with a $\mathbf{E}^3$dependence, respectively. It is important to note that the development of the E_{EEC} parameter [55] is valid for negatively charged particles that satisfy this condition: $|\zeta_P| < |\zeta_W|$, in the microchannel that also possesses a negative ζ_W; this condition is fulfilled by many polystyrene microparticles and cells employed in these systems. A positively charged particle or a negatively charged particle with $|\zeta_P| > |\zeta_W|$ will not reach $\mathbf{v}_P = 0$ as required for E_{EEC} determination. Only a handful of recent reports [54–56] include the experimental characterization of $\mu_{EP}^{(3)}$. The E_{EEC} parameter has potential to be used as a unique EK signature for the rapid identification of microparticles and microorganisms that possess a negative charge and fulfill this condition $|\zeta_P| < |\zeta_W|$. Significant efforts have been dedicated to identifying an electrical phenotype for microorganisms [178, 179]; the E_{EEC} parameter may be the answer to these efforts, since for the first time in the field of DC-iEK systems, the effects of EP of the second kind are being taken into account.

Besides trapping, successful particle separation and enrichment by continuous sorting or continuous focusing were achieved by employing the migration regime of particle streaming as identified by Cummings [76, 77]. The Xuan group has made numerous major contributions to the development of this continuous particle separation methodology, in particular by developing devices with curved walls [153–160]. For devices that use the streaming particle migration regime, the following expression for particle velocity has been proposed by the Xuan group [128, 129], where λ is the correction factor, which was in the range of 0.6 to 0.8 for polystyrene microparticles.

$$\mathbf{v}_P = \mathbf{v}_{EK} + \lambda\mathbf{v}_{DEP}, \text{where} : \mathbf{v}_{EK} = \mathbf{v}_{EO} + \mathbf{v}_{EP}^{(1)} \quad (15)$$

Considering these recent findings [43, 54–56], it is proposed to rename the field formerly known as DC-iDEP with the new name of DC-iEK; analogously, the field of low-frequency AC-iDEP should be called low-frequency AC-iEK (see next section). These recent reports suggest that EP of the second kind was present in the studies referenced in the previous section of this article, but its effects were perhaps identified as negative DEP, which led to the use of correction factors [175]. As stated recently by Perez-Gonzalez, not considering the effects of EP of the second kind may also explain why positive DEP was never observed in DC-iDEP systems [39].

The new field of direct current insulator–based electrokinetic (DC-iEK) devices

In a recent report from our group [58] where we studied the trapping of bacterial and yeast cells in PDMS devices with insulating posts, it was identified that the contribution of DEP to the total particle velocity was only 5.85% of that of EP of the second kind under the conditions of particle trapping. This means that DEP, although present, is not a dominant effect when compared to both EP effects and EO flow. These findings further support the work by Tottori et al. [54] and Cardenas-Benitez et al. [55] that proposed that DEP was not the dominant phenomenon responsible for particle trapping in DC-iEK systems, and that particle trapping is mainly the result of an equilibrium between EO flow and EP forces (linear and nonlinear). Figure 7 illustrates the new representation of forces exerted on a negatively charged particle in DC-iEK and low-frequency(< 1 kHz)AC-iEK devices with arrays of insulating posts, where, for the first time, both linear and nonlinear EP effects are considered, along with EO flow and a *smaller* DEP force.

The identification of the significant effects of EP of the second kind has initiated a new and exciting new area in

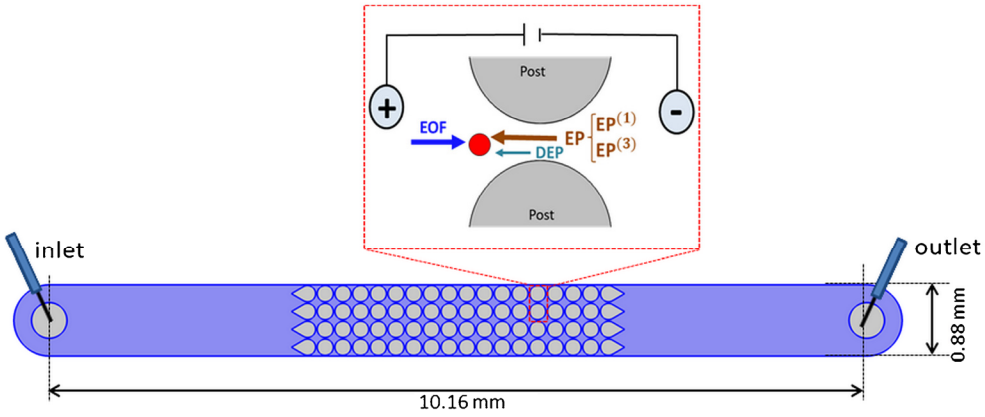

Fig. 7 Illustration of the forces present in a DC-iEK device with cylindrical insulating posts for a negatively charged particle with $|\zeta_P| < |\zeta_W|$, in a channel with a negative zeta potential, considering both linear and nonlinear EP, EO flow, and DEP, where DEP is depicted as a *smaller* force compared to the two EP forces (linear and nonlinear)

microscale EK separations. The new parameter of E_{EEC} holds great promise to be used as a unique EK signature [14, 58] for rapid identification of microorganisms. By including EP of the second kind in mathematical models, it is now possible to predict particle EK migration in DC-iEK systems in a more accurate manner than before, without the need of correction factors [175]. It is believed that EP of the second kind was the missing piece of information that prevented accurate modeling of particle EK migration in these systems. As recently stated [59], the effects of nonlinear EP had been previously predicted theoretically by several studies [42, 47, 49, 50, 53], and the new contributions [43, 54–56] provide the much needed experimental demonstration. New studies that consider EP of the second kind in DC-iEK systems are now being published [11, 39, 57, 152, 180], supporting the findings in these recent reports [43, 54–56] and demonstrating the enthusiasm motivated by this potential major change in our understanding of DC-iEK systems.

Concluding remarks

This is an exciting time in the field of iEK microsystems under DC and low-frequency(< 1 kHz) AC fields. The recent experimental findings reported by several groups [43, 54–56] support the theory that the nonlinear EK phenomenon of EP of the second kind plays a major role in particle migration and particle trapping in these systems. Considering these findings, particle trapping is mainly the result of the balance between EO flow and EP forces (linear and nonlinear), as demonstrated by Tottori et al. [54] and Cardenas-Benitez et al. [55], and not a product of DEP forces as it has been believed for two decades, since the reports by Cummings et al. [74–77]. This new proposed theory seems to explain the discrepancy between experimental and predicted DEP forces that was identified by the Hayes group in 2011 [117], where experimentally measured DEP mobilities were lower than what was required to achieve particle trapping. Furthermore, this new theory, that considers EP of the second kind may also explain the discrepancy between experimental and modeling results that gave rise to the use of correction factors in the models [175] and originated the search for expressions for the trapping condition [126, 172], electrokinetic ratio [123, 124], and the trapping value [105] to describe particle trapping. Although these modeling efforts [105, 123, 124, 126, 172, 175] advanced our understanding of the mechanism behind particle trapping, it was necessary to bring together the knowledge reported by many researchers in the field of physics and colloids [42, 45–51] to the field of microscale EK separations [43, 54–56] to finally understand the forces behind particle trapping.

Much research is still needed, in particular, the effects of EO of the second kind must be investigated as nonlinear EO flow might also play a role in these systems, as reported by the Xuan [59] and Buie [60] research groups. Another aspect that must be addressed is the high voltage requirement [84], which is an impediment for the miniaturization of these systems, which also limits the choice of suspending media to be used to low-conductivity media. Strategies for reducing voltage requirements have been proposed by the Ros [108] and Swami [132, 133] groups with the use of nano constrictions. Despite these particular challenges and other drawbacks not mentioned here, these new findings of the effects of EP of the second kind open new opportunities in the field of microscale EK separations. By considering both linear and nonlinear EP effects on particle migration, it may be possible to now develop, for the first time, more accurate mathematical models that will allow precise predictions of the conditions necessary for particle trapping. Only a few recent reports [54–56] are available in the literature that report the experimental characterization of the nonlinear EP mobility of particles (and cells) with a $\mathbf{E}^3$ dependence ($\mu_{EP}^{(3)}$); more studies are needed aimed to characterize particles and microorganisms in terms of their linear and nonlinear EK migration, so their behavior can be accurately modeled. As a summary statement, this review article describes the start and evolution of the field of DC-iEK(and low frequency AC-iEK) systems; it also describes an important recent change, where the effects of EP of the second kind were identified as a major force influencing particle migration.

Dielectrophoresis is still a force present in these systems, but as demonstrated by recent reports [54, 55, 58], DEP seems not to be a dominant force in systems stimulated by DC and low-frequency(< 1 kHz) AC potentials. Of course, this assessment needs to be applied with caution, as the system performance depends on the specific operating conditions. The relative effects of EP of the second kind and DEP must be evaluated for each system, as it is not possible to assume that DEP is always negligible and that EP of the second kind is always significant. The recent reports [43, 54–56] have unveiled new and exciting findings, but much more research is still needed. Finally, the author of this review article considers that renaming this field from DC-iDEP to DC-iEK provides a more accurate description of the several EK phenomena (not only DEP) behind particle manipulation and trapping in insulator-based EK systems.

Acknowledgements The author would like to acknowledge the financial support provided by the National Science Foundation (CBET- 1705895).

Declaration

Conflict of interest The author declares no competing interests.

Ethical approval This article does not contain any studies with human participants or animals.

Informed consent Informed consent is not applicable in this study.

References

1. Whitesides GM. The origins and the future of microfluidics. Nature. 2006;442:368–73.
2. Hughes MP. Nanoelectromechanics in engineering and biology, 1st ed. Nanoelectromechanics Eng Biol. 2002. https://doi.org/10.1201/9781315219202.
3. Oh M, Jayasooriya V, Woo SO, Nawarathna D, Choi Y. Selective manipulation of biomolecules with insulator-based dielectrophoretic tweezers. ACS Appl Nano Mater. 2020;3:797–805.
4. Modarres P, Tabrizian M. Alternating current dielectrophoresis of biomacromolecules: the interplay of electrokinetic effects. Sensors Actuators B Chem. 2017;252:391–408.
5. Jones PV, Salmon GL, Ros A. Continuous separation of DNA molecules by size using insulator-based dielectrophoresis. Anal Chem. 2017;89:1531–9.
6. Lapizco-Encinas BH. Microscale electrokinetic assessments of proteins employing insulating structures. Curr Opin Chem Eng. 2020;29:9–16.
7. Hayes MA. Dielectrophoresis of proteins: experimental data and evolving theory. Anal Bioanal Chem. 2020;412:3801–11.
8. Coll De Peña A, Mohd Redzuan NH, Abajorga M, Hill N, Thomas JA, Lapizco-Encinas BH. Analysis of bacteriophages with insulator-based dielectrophoresis. Micromachines. 2019;10:450.
9. Madiyar FR, Haller SL, Farooq O, Rothenburg S, Culbertson C, Li J. AC dielectrophoretic manipulation and electroporation of vaccinia virus using carbon nanoelectrode arrays. Electrophoresis. 2017;38:1515–25.
10. Hakim KS, Lapizco-Encinas BH. Analysis of microorganisms with nonlinear electrokinetic microsystems. Electrophoresis. 2021;42:588–604.
11. Hill N, De Peña AC, Miller A, Lapizco-Encinas BH. On the potential of microscale electrokinetic cascade devices. Electrophoresis. 2021. https://doi.org/10.1002/elps.202100069.
12. Kumar N, Wang W, Ortiz-Marquez JC, et al. Dielectrophoresis assisted rapid, selective and single cell detection of antibiotic resistant bacteria with G-FETs. Biosens Bioelectron. 2020;156:112123.
13. Moore JH, Honrado C, Stagnaro V, Kolling G, Warren CA, Swami NS. Rapid in vitro assessment of Clostridioides difficile inhibition by probiotics using dielectrophoresis to quantify cell structure alterations. ACS Infect Dis. 2020;6:1000–7.
14. Coll De Peña A, Hill N, Lapizco-Encinas BH. Determination of the empirical electrokinetic equilibrium condition of microorganisms in microfluidic devices. Biosensors. 2020;10:148.
15. Ettehad HM, Zarrin PS, Hölzel R, Wenger C. Dielectrophoretic immobilization of yeast cells using CMOS integrated microfluidics. Micromachines. 2020;11:501.
16. Ho B, Beech J, Tegenfeldt J. Cell sorting using electrokinetic deterministic lateral displacement. Micromachines. 2020;12:30.
17. Çağlayan Z, Demircan Yalçın Y, Külah H. Examination of the dielectrophoretic spectra of MCF7 breast cancer cells and leukocytes. Electrophoresis. 2020;41:345–52.
18. Ringwelski B, Jayasooriya V, Nawarathna D. Dielectrophoretic high purity isolation of primary T-cells in samples contaminated with leukemia cells, for biomanufacturing of therapeutic CAR T-cells. J Phys D Appl Phys. 2020;54:10.
19. Zahedi Siani O, Zabetian Targhi M, Sojoodi M, Movahedin M. Dielectrophoretic separation of monocytes from cancer cells in a microfluidic chip using electrode pitch optimization. Bioprocess Biosyst Eng. 2020;43:1573–86.
20. Aghaamoo M, Aghilinejad A, Chen X, Xu J. On the design of deterministic dielectrophoresis for continuous separation of circulating tumor cells from peripheral blood cells. Electrophoresis. 2019;40:1486–93.
21. Chuang HS, Raizen DM, Lamb A, Dabbish N, Bau HH. Dielectrophoresis of Caenorhabditis elegans. Lab Chip. 2011;11:599–604.
22. Rezai P, Siddiqui A, Selvaganapathy PR, Gupta BP. Behavior of Caenorhabditis elegans in alternating electric field and its application to their localization and control. Appl Phys Lett. 2010;96:153702.
23. Keck D, Stuart C, Duncan J, Gullette E, Martinez-Duarte R. Highly localized enrichment of Trypanosoma brucei parasites using dielectrophoresis. Micromachines. 2020;11:625.
24. O'Konski CT. Electric properties of macromolecules. V Theory of ionic polarization in polyelectrolytes. J Phys Chem. 1960;64:605–19.
25. Das S, Chakraborty S. Transport and separation of charged macromolecules under nonlinear electromigration in nanochannels. Langmuir. 2008;24:7704–10.
26. Kłodzińska E, Buszewski B. Electrokinetic detection and characterization of intact microorganisms. Anal Chem. 2009;81:8–15.
27. Polaczyk AL, Amburgey JE, Alansari A, Poler JC, Propato M, Hill VR. Calculation and uncertainty of zeta potentials of microorganisms in a 1:1 electrolyte with a conductivity similar to surface water. Colloids Surf A Physicochem Eng Asp. 2020;586:124097.
28. Fernandez RE, Rohani A, Farmehini V, Swami NS. Review: microbial analysis in dielectrophoretic microfluidic systems. Anal Chim Acta. 2017;966:11–33.

29. Lapizco-Encinas BH. Microscale nonlinear electrokinetics for the analysis of cellular materials in clinical applications: a review. Microchim Acta. 2021;188:104.
30. Douglas TA, Cemazar J, Balani N, Sweeney DC, Schmelz EM, Davalos RV. A feasibility study for enrichment of highly aggressive cancer subpopulations by their biophysical properties via dielectrophoresis enhanced with synergistic fluid flow. Electrophoresis. 2017;38:1507–14.
31. Alinezhadbalalami N, Douglas TA, Balani N, Verbridge SS, Davalos RV. The feasibility of using dielectrophoresis for isolation of glioblastoma subpopulations with increased stemness. Electrophoresis. 2019;40:2592–600.
32. Manczak R, Saada S, Provent T, et al. UHF-dielectrophoresis crossover frequency as a new marker for discrimination of glioblastoma undifferentiated cells. IEEE J Electromagn RF Microwaves Med Biol. 2019;3:191–8.
33. Trainito CI, Sweeney DC, Čemažar J, Schmelz EM, Français O, Le Pioufle B, Davalos RV. Characterization of sequentially-staged cancer cells using electrorotation. PLoS One. 2019;14:1–18.
34. Keim K, Rashed MZ, Kilchenmann SC, Delattre A, Gonçalves AF, Éry P, Guiducci C. On-chip technology for single-cell arraying, electrorotation-based analysis and selective release. Electrophoresis. 2019;40:1830–8.
35. Thiriet P-E, Pezoldt J, Gambardella G, Keim K, Deplancke B, Guiducci C. Selective retrieval of individual cells from microfluidic arrays combining dielectrophoretic force and directed hydrodynamic flow. Micromachines. 2020;11:322.
36. Jayasooriya VD, Nawarathna D. Label-free purification of viable human T-lymphocyte cells from a mixture of viable and nonviable cells after transfection by electroporation. J Phys D Appl Phys. 2019;52:36LT01.
37. Xuan X. Recent advances in direct current electrokinetic manipulation of particles for microfluidic applications. Electrophoresis. 2019;40:2484–513.
38. Lapizco-Encinas BH. On the recent developments of insulator-based dielectrophoresis: a review. Electrophoresis. 2019;40:358–75.
39. Perez-Gonzalez VH. Particle trapping in electrically driven insulator-based microfluidics: Dielectrophoresis and induced-charge electrokinetics. Electrophoresis. 2021. https://doi.org/10.1002/elps.202100123.
40. Mishchuk NA, Dukhin SS. Electrophoresis of solid particles at large Peclet numbers. Electrophoresis. 2002;23:2012–22.
41. Mishchuk NA, Takhistov PV. Electroosmosis of the second kind. Colloids Surf A Physicochem Eng Asp. 1995;95:119–31.
42. Dukhin SS. Electrokinetic phenomena of the second kind and their applications. Adv Colloid Interf Sci. 1991;35:173–96.
43. Rouhi Youssefi M, Diez FJ. Ultrafast electrokinetics. Electrophoresis. 2016;37:692–8.
44. Dukhin AS, Ulberg ZR, Gruzina TG, Karamushka VI. Peculiarities of live cells' interaction with micro- and nanoparticles. In: Colloid Interface Sci. Pharm: Res. Dev. Elsevier Inc.; 2014. p. 193–222.
45. Dukhin SS. Non-equilibrium electric surface phenomena. Adv Colloid Interf Sci. 1993;44:1–134.
46. Mishchuk NA, Barinova NO. Theoretical and experimental study of nonlinear electrophoresis. Colloid J. 2011;73:88–96.
47. Mishchuk NA. Concentration polarization of interface and nonlinear electrokinetic phenomena. Adv Colloid Interf Sci. 2010;160:16–39.
48. Shilov V, Barany S, Grosse C, Shramko O. Field-induced disturbance of the double layer electro-neutrality and non-linear electrophoresis. Adv Colloid Interf Sci. 2003;104:159–73.
49. Schnitzer O, Zeyde R, Yavneh I, Yariv E. Weakly nonlinear electrophoresis of a highly charged colloidal particle. Phys Fluids. 2013;25:052004.
50. Schnitzer O, Yariv E. Nonlinear electrophoresis at arbitrary field strengths: small-Dukhin-number analysis. Phys Fluids. 2014;26:122002.
51. Schnitzer O, Yariv E. Macroscale description of electrokinetic flows at large zeta potentials: nonlinear surface conduction. Phys Rev E - Stat Nonlinear, Soft Matter Phys. 2012;86:021503.
52. Khair AS. Strong deformation of the thick electric double layer around a charged particle during sedimentation or electrophoresis. Langmuir. 2018;34:876–85.
53. Barany S. Electrophoresis in strong electric fields. Adv Colloid Interf Sci. 2009;147–148:36–43.
54. Tottori S, Misiunas K, Keyser UF, Bonthuis DJ. Nonlinear electrophoresis of highly charged nonpolarizable particles. Phys Rev Lett. 2019;123:14502.
55. Cardenas-Benitez B, Jind B, Gallo-Villanueva RC, Martinez-Chapa SO, Lapizco-Encinas BH, Perez-Gonzalez VH. Direct current electrokinetic particle trapping in insulator-based microfluidics: theory and experiments. Anal Chem. 2020;92:12871–9.
56. Antunez-Vela S, Perez-Gonzalez VH, Coll De Peña A, Lentz CJ, Lapizco-Encinas BH. Simultaneous determination of linear and nonlinear electrophoretic mobilities of cells and microparticles. Anal Chem. 2020;92:14885–91.
57. Quevedo DF, Lentz CJ, Coll De Peña A, Hernandez Y, Habibi N, Rikako M, Lahann J, Lapizco-Encinas BH. Electrokinetic characterization of synthetic protein nanoparticles. Beilstein J Nanotechnol. 2020;11:1556–67.
58. Coll De Peña A, Miller A, Lentz CJ, Hill N, Parthasarathy A, Hudson AO, Lapizco-Encinas BH. Creation of an electrokinetic characterization library for the detection and identification of biological cells. Anal Bioanal Chem. 2020;412:3935–45.
59. Xuan X. Review of nonlinear electrokinetic flows in insulator-based dielectrophoresis: from induced charge to joule heating effects. Electrophoresis. 2021. https://doi.org/10.1002/ELPS.202100090.
60. Qianru W, Neehar DN, R. BC, Wang Q, Dingari NN, Buie CR. Nonlinear electrokinetic effects in insulator-based dielectrophoretic systems. Electrophoresis. 2017;38:2576–86.
61. Pohl HA. The motion and precipitation of Suspensoids in divergent electric fields. J Appl Phys. 1951;22:869–71.
62. Pohl HA, Schwar JP. Factors affecting separation of suspensions in nonuniform electric fields. J Appl Phys. 1959;30:69–73.
63. Pohl HA, Schwar JP. Particle separations by nonuniform electric fields in liquid dielectrics, batch methods. J Electrochem Soc. 1960;107:383–95.
64. Pohl HA, Hawk I (1966) Separation of living and dead cells by dielectrophoresis. Science (80-) 152:647–649.
65. Crane JS, Pohl HA. A study of living and dead yeast cells using dielectrophoresis. J Electrochem Soc. 1968;115:584–6.
66. Pohl HA, Crane JS. Dielectrophoresis of cells. Biophys J. 1971;11:711–27.
67. Pohl HA. Dielectrophoresis. Cambridge: Cambridge University Press; 1978.
68. Pohl HA, Pohl HA. Dielectrophoresis: the behavior of neutral matter in nonuniform electric fields: Cambridge university press Cambridge; 1978.
69. Hughes MP. Fifty years of dielectrophoretic cell separation technology. Biomicrofluidics. 2016;10:032801. https://doi.org/10.1063/1.4954841.
70. Pethig R. Dielectrophoresis: status of the theory, technology, and applications. Biomicrofluidics. 2010;4:022811.
71. Pethig R. Dielectrophoresis: using inhomogeneous AC electrical fields to separate and manipulate cells. Crit Rev Biotechnol. 1996;16:331–48.

72. Masuda S, Washizu M, Nanba T. Novel method of cell fusion in field constriction area in fluid integrated circuit. IEEE Trans Ind Appl. 1989;25:732–7.
73. Gel M, Kimura Y, Kurosawa O, Oana H, Kotera H, Washizu M. Dielectrophoretic cell trapping and parallel one-to-one fusion based on field constriction created by a micro-orifice array. Biomicrofluidics. 2010;4:22808.
74. Cummings EB, Singh AK. Dielectrophoretic trapping without embedded electrodes. In: Becker H, editor. Mastrangelo CH. CA: Proc. SPIE. Santa Clara; 2000. p. 151–60.
75. Cummings EB (2002) A comparison of theoretical and experimental electrokinetic and dielectrophoretic flow fields. In: 32nd AIAA Fluid Dyn. Conf. Exhib. 2002. American Institute of Aeronautics and Astronautics, St. Louis, Missouri, pp. 1–17.
76. Cummings EB, Singh AK. Dielectrophoresis in microchips containing arrays of insulating posts: theoretical and experimental results. Anal Chem. 2003;75:4724–31.
77. Cummings EB. Streaming dielectrophoresis for continuous-flow microfluidic devicc. IEEE Eng Med Biol Mag. 2003;22:75–84.
78. Lapizco-Encinas BH, Simmons BA, Cummings EB, Fintschenko Y. Dielectrophoretic concentration and separation of live and dead Bacteria in an array of insulators. Anal Chem. 2004;76:1571–9.
79. Lapizco-Encinas BH, Simmons BA, Cummings EB, Fintschenko Y. Insulator-based dielectrophoresis for the selective concentration and separation of live bacteria in water. Electrophoresis. 2004;25:1695–704.
80. Lapizco-Encinas BH, Davalos R V., Simmons BA, Cummings EB, Fintschenko Y. An insulator-based(electrodeless) dielectrophoretic concentrator for microbes in water. In: J. Microbiol. Methods. 2005;62:317–326.
81. Gallo-Villanueva RC, Rodríguez-López CE, Díaz-de-la-Garza RI, Reyes-Betanzo C, Lapizco-Encinas BH. DNA manipulation by means of insulator-based dielectrophoresis employing direct current electric fields. Electrophoresis. 2009;30:4195–205.
82. Chou CF, Tegenfeldt JO, Bakajin O, Chan SS, Cox EC, Darnton N, Duke T, Austin RH. Electrodeless dielectrophoresis of single- and double-stranded DNA. Biophys J. 2002;83:2170–9.
83. Chou CF, Zenhausern F. Electrodeless dielectrophoresis for micro total analysis systems. IEEE Eng Med Biol Mag. 2003;22:62–7.
84. Ramirez-Murillo CJ, de los Santos-Ramirez JM, Perez-Gonzalez VH. Toward low-voltage dielectrophoresis-based microfluidic systems: a review. Electrophoresis. 2021;42:565–587.
85. Benhal P, Quashie D, Kim Y, Ali J. Insulator based dielectrophoresis: Micro, nano, and molecular scale biological applications. Scnsors (Switzcrland). 2020;20:1–24.
86. Saucedo-Espinosa MA, Lapizco-Encinas BH. Experimental and theoretical study of dielectrophoretic particle trapping in arrays of insulating structures: effect of particle size and shape. Electrophoresis. 2015;36:1086–97.
87. Mela P, van den Berg A, Fintschenko Y, Cummings EB, Simmons BA, Kirby BJ. The zeta potential of cyclo-olefin polymer microchannels and its effects on insulative (electrodeless) dielectrophoresis particle trapping devices. Electrophoresis. 2005;26:1792–9.
88. Braff WA, Pignier A, Buie CR. High sensitivity three-dimensional insulator-based dielectrophoresis. Lab Chip. 2012;12:1327–31.
89. Lapizco-Encinas BH, Ozuna-Chacón S, Rito-Palomares M. Protein manipulation with insulator-based dielectrophoresis and direct current electric fields. J Chromatogr A. 2008;1206:45–51.
90. Gallo-Villanueva RC, Jesús-Pérez NM, Martínez-López JI, Pacheco A, Lapizco-Encinas BH. Assessment of microalgae viability employing insulator-based dielectrophoresis. Microfluid Nanofluid. 2011;10:1305–15.
91. LaLonde A, Romero-Creel MF, Saucedo-Espinosa MA, Lapizco-Encinas BH. Isolation and enrichment of low abundant particles with insulator-based dielectrophoresis. Biomicrofluidics. 2015;9:064113.
92. Saucedo-Espinosa MA, Lalonde A, Gencoglu A, Romero-Creel MF, Dolas JR, Lapizco-Encinas BH. Dielectrophoretic manipulation of particle mixtures employing asymmetric insulating posts. Electrophoresis. 2016;37:282–90.
93. Gencoglu A, Olney D, Lalonde A, Koppula KS, Lapizco-Encinas BH. Dynamic microparticle manipulation with an electroosmotic flow gradient in low-frequency alternating current dielectrophoresis. Electrophoresis. 2014;35:362–73.
94. Romero-Creel MF, Goodrich E, Polniak DV, Lapizco-Encinas BH. Assessment of sub-micron particles by exploiting charge differences with dielectrophoresis. Micromachines. 2017. https://doi.org/10.3390/mi8080239.
95. Saucedo-Espinosa MA, Rauch MM, Lalonde A, Lapizco-Encinas BH. Polarization behavior of polystyrene particles under direct current and low-frequency (<1 kHz) electric fields in dielectrophoretic systems. Electrophoresis. 2016;37:635–44.
96. IIill N, Lapizco-Encinas BII. Continuous flow separation of particles with insulator-based dielectrophoresis chromatography. Anal Bioanal Chem. 2020;412:3891–902.
97. LaLonde A, Gencoglu A, Romero-Creel MF, Koppula KS, Lapizco-Encinas BH. Effect of insulating posts geometry on particle manipulation in insulator based dielectrophoretic devices. J Chromatogr A. 2014;1344:99–108.
98. Saucedo-Espinosa MA, Lapizco-Encinas BH. Design of insulator-based dielectrophoretic devices: effect of insulator posts characteristics. J Chromatogr A. 2015;1422:325–33.
99. Perez-Gonzalez VH, Gallo-Villanueva RC, Cardenas-Benitez B, Martinez-Chapa SO, Lapizco-Encinas BH. Simple approach to reducing particle trapping voltage in insulator-based dielectrophoretic systems. Anal Chem. 2018;90:4310–5.
100. Lentz CJ, Hidalgo-Caballero S, Lapizco-Encinas BH. Low frequency cyclical potentials for fine tuning insulator-based dielectrophoretic separations. Biomicrofluidics. 2019;13:044114.
101. Mata-Gomez MA, Perez-Gonzalez VH, Gallo-Villanueva RC, Gonzalez-Valdez J, Rito-Palomares M, Martinez-Chapa SO. Modelling of electrokinetic phenomena for capture of PEGylated ribonuclease a in a microdevice with insulating structures. Biomicrofluidics. 2016;10:33106.
102. Ayala-Mar S, Perez-Gonzalez VH, Mata-Gómez MA, Gallo-Villanueva RC, Gonzalez-Valdez J. Electrokinetically driven exosome separation and concentration using dielectrophoretic-enhanced PDMS-based microfluidics. Anal Chem. 2019;91:14975–82.
103. Pesch GR, Kiewidt L, Du F, Baune M, Thöming J. Electrodeless dielectrophoresis: impact of geometry and material on obstacle polarization. Electrophoresis. 2016;37:291–301.
104. Pesch GR, Du F, Baune M, Thöming J. Influence of geometry and material of insulating posts on particle trapping using positive dielectrophoresis. J Chromatogr A. 2017;1483:127–37.
105. Mohammadi M, Zare MJ, Madadi H, Sellarès J, Casals-Terré J. A new approach to design an efficient micropost array for enhanced direct-current insulator-based dielectrophoretic trapping. Anal Bioanal Chem. 2016;408:5285–94.
106. Gan L, Chao T-CC, Camacho-Alanis F, Ros A. Six-helix bundle and triangle DNA origami insulator-based dielectrophoresis. Anal Chem. 2013;85:11427–34.
107. Nakano A, Chao T-CC, Camacho-Alanis F, Ros A. Immunoglobulin G and bovine serum albumin streaming dielectrophoresis in a microfluidic device. Electrophoresis. 2011;32:2314–22.
108. Nakano A, Camacho-Alanis F, Ros A. Insulator-based dielectrophoresis with [small beta]-galactosidase in nanostructured devices. Analyst. 2015;140:860–8.

109. Rabbani MT, Schmidt CF, Ros A. Single-walled carbon nanotubes probed with insulator-based dielectrophoresis. Anal Chem. 2017;89:13235–44.
110. Luo J, Abdallah BG, Wolken GG, Arriaga EA, Ros A. Insulator-based dielectrophoresis of mitochondria. Biomicrofluidics. 2014;8:1–11.
111. Bhattacharya S, Chao T-CC, Ros A. Insulator-based dielectrophoretic single particle and single cancer cell trapping. Electrophoresis. 2011;32:2550–8.
112. Bhattacharya S, Chao T-CC, Ariyasinghe N, Ruiz Y, Lake D, Ros R, Ros A. Selective trapping of single mammalian breast cancer cells by insulator-based dielectrophoresis. Anal Bioanal Chem. 2014;406:1855–65.
113. Calero V, Garcia-Sanchez P, Ramos A, Morgan H. Combining DC and AC electric fields with deterministic lateral displacement for micro- and nano-particle separation. Biomicrofluidics. 2019;13:054110.
114. Calero V, Garcia-Sanchez P, Honrado C, Ramos A, Morgan H. AC electrokinetic biased deterministic lateral displacement for tunable particle separation. Lab Chip. 2019;19:1386–96.
115. Calero V, García-Sánchez P, Ramos A, Morgan H. Electrokinetic biased deterministic lateral displacement: scaling analysis and simulations. J Chromatogr A. 1623;2020:461151.
116. Pysher MD, Hayes MA. Electrophoretic and dielectrophoretic field gradient technique for separating bioparticles. Anal Chem. 2007;79:4552–7.
117. Weiss NG, Jones PV, Mahanti P, Chen KP, Taylor TJ, Hayes MA. Dielectrophoretic mobility determination in DC insulator-based dielectrophoresis. Electrophoresis. 2011;32:2292–7.
118. Crowther CV, Sanderlin V, Hayes MA, Gile GH. Effects of surface treatments on trapping with DC insulator-based dielectrophoresis. Analyst. 2019;144:7478–88.
119. Jones PV, DeMichele AF, Kemp LK, Hayes MA. Differentiation of Escherichia coli serotypes using DC gradient insulator dielectrophoresis. Anal Bioanal Chem. 2014;406:183–92.
120. Ding J, Lawrence RM, Jones PV, Hogue BG, Hayes MA. Concentration of Sindbis virus with optimized gradient insulator-based dielectrophoresis. Analyst. 2016;141:1997–2008.
121. Jones PV, Staton SJR, Hayes MA. Blood cell capture in a sawtooth dielectrophoretic microchannel. Anal Bioanal Chem. 2011;401:2103–11.
122. Staton SJRR, Chen KP, Taylor TJ, Pacheco JR, Hayes MA. Characterization of particle capture in a sawtooth patterned insulating electrokinetic microfluidic device. Electrophoresis. 2010;31:3634–41.
123. Crowther CV, Hilton SH, Kemp LK, Hayes MA. Isolation and identification of *listeria monocytogenes* utilizing DC insulator-based dielectrophoresis. Anal Chim Acta. 2019;1068:41–51.
124. Liu Y, Jiang A, Kim E, Ro C, Adams T, Flanagan LA, Taylor TJ, Hayes MA. Identification of neural stem and progenitor cell subpopulations using DC insulator-based dielectrophoresis. Analyst. 2019;144:4066–72.
125. Jones PV, Hayes MA. Development of the resolution theory for gradient insulator-based dielectrophoresis. Electrophoresis. 2015;36:1098–106.
126. Crowther CV, Hayes MA. Refinement of insulator-based dielectrophoresis. Analyst. 2017;142:1608–18.
127. Weirauch L, Lorenz M, Hill N, Lapizco-Encinas BH, Baune M, Pesch GR, Thöming J. Material-selective separation of mixed microparticles via insulator-based dielectrophoresis. Biomicrofluidics. 2019;13:064112.
128. Lu S-YY, Malekanfard A, Beladi-Behbahani S, Zu W, Kale A, Tzeng T-RR, Wang Y-NN, Xuan X. Passive dielectrophoretic focusing of particles and cells in ratchet microchannels. Micromachines. 2020;11:451.
129. Malekanfard A, Beladi-Behbahani S, Tzeng T-R, Zhao H, Xuan X. AC insulator-based dielectrophoretic focusing of particles and cells in an "infinite" microchannel. Anal Chem. 2021;93:5947–53.
130. Malekanfard A, Liu Z, Song L, Kale A, Zhang C, Yu L, Song Y, Xuan X. Joule heating-enabled electrothermal enrichment of nanoparticles in insulator-based dielectrophoretic microdevices. Electrophoresis. 2021;42:626–34.
131. Bentor J, Malekanfard A, Raihan MK, Wu S, Pan X, Song Y, Xuan X. Insulator-based dielectrophoretic focusing and trapping of particles in non-Newtonian fluids. Electrophoresis. 2021;00:1–8.
132. Liao K-TT, Tsegaye M, Chaurey V, Chou C-FF, Swami NS. Nano-constriction device for rapid protein preconcentration in physiological media through a balance of electrokinetic forces. Electrophoresis. 2012;33:1958–66.
133. Sanghavi BJ, Varhue W, Rohani A, Liao K-TT, Bazydlo LALL, Chou C-FF, Swami NS. Ultrafast immunoassays by coupling dielectrophoretic biomarker enrichment in nanoslit channel with electrochemical detection on graphene. Lab Chip. 2015;15:4563–70.
134. Swami N, Chou C-FF, Ramamurthy V, Chaurey V. Enhancing DNA hybridization kinetics through constriction-based dielectrophoresis. Lab Chip. 2009;9:3212–20.
135. Mohammadi M, Madadi H, Casals-Terré J, Sellarès J. Hydrodynamic and direct-current insulator-based dielectrophoresis (H-DC-iDEP) microfluidic blood plasma separation. Anal Bioanal Chem. 2015;407:4733–44.
136. Hyoung Kang K, Xuan X, Kang Y, Li D, Kang KH, Xuan X, Kang Y, Li D. Effects of dc-dielectrophoretic force on particle trajectories in microchannels. J Appl Phys. 2006;99:64702–8.
137. Kang KH, Kang Y, Xuan X, Li D. Continuous separation of microparticles by size with direct current-dialectrophoresis. Electrophoresis. 2006;27:694–702.
138. Kang Y, Li D, Kalams SA, Eid JE. DC-dielectrophoretic separation of biological cells by size. Biomed Microdevices. 2008;10:243–9.
139. Kang Y, Cetin B, Wu Z, Li D. Continuous particle separation with localized AC-dielectrophoresis using embedded electrodes and an insulating hurdle. Electrochim Acta. 2009;54:1715–20.
140. Hawkins BG, Kirby BJ. Electrothermal flow effects in insulating (electrodeless) dielectrophoresis systems. Electrophoresis. 2010;31:3622–33.
141. Srivastava SK, Baylon-Cardiel JL, Lapizco-Encinas BH, Minerick AR. A continuous DC-insulator dielectrophoretic sorter of microparticles. J Chromatogr A. 2011;1218:1780–9.
142. Srivastava SK, Artemiou A, Minerick AR. Direct current insulator-based dielectrophoretic characterization of erythrocytes: ABO-Rh human blood typing. Electrophoresis. 2011;32:2530–40.
143. Abdallah BG, Roy-Chowdhury S, Coe J, et al. Microfluidic sorting of protein nanocrystals by size for X-ray free-electron laser diffraction. Struct Dyn. 2015;2:41719.
144. Abdallah BG, Roy-Chowdhury S, Coe J, Fromme P, Ros A. High throughput protein nanocrystal fractionation in a microfluidic sorter. Anal Chem. 2015;87:4159–67.
145. Zhu J, Xuan X. Dielectrophoretic focusing of particles in a microchannel constriction using DC-biased AC flectric fields. Electrophoresis. 2009;30:2668–75.
146. Patel S, Qian S, Xuan X. Reservoir-based dielectrophoresis for microfluidic particle separation by charge. Electrophoresis. 2013;34:961–8.
147. Kale A, Patel S, Xuan X. Three-dimensional reservoir-based Dielectrophoresis (rDEP) for enhanced particle enrichment. Micromachines. 2018;9:123.

148. Shi L, Esfandiari L. An Electrokinetically-driven microchip for rapid entrapment and detection of nanovesicles. Micromachines. 2020;12:11.
149. Braff WA, Willner D, Hugenholtz P, Rabaey K, Buie CR. Dielectrophoresis-based discrimination of bacteria at the strain level based on their surface properties. PLoS One. 2013;8:e76751.
150. Wang Q, Jones A-ADAD, Gralnick JA, Lin L, Buie CR. Microfluidic dielectrophoresis illuminates the relationship between microbial cell envelope polarizability and electrochemical activity. Sci Adv. 2019;5:eaat5664.
151. Pudasaini S, Perera ATK, Das D, Ng SH, Yang C. Continuous flow microfluidic cell inactivation with the use of insulating micropillars for multiple electroporation zones. Electrophoresis. 2019;40:2522–9.
152. Pudasaini S, Perera ATK, Ng SH, Yang C. Bacterial inactivation via microfluidic electroporation device with insulating micropillars. Electrophoresis. 2021;42:1093–101.
153. Church C, Zhu JJ, Wang GY, Tzeng TRJ, Xuan XC. Electrokinetic focusing and filtration of cells in a serpentine microchannel. Biomicrofluidics. 2009;3:44109–10.
154. Zhu J, Tzeng TRJ, Hu G, Xuan X. DC dielectrophoretic focusing of particles in a serpentine microchannel. Microfluid Nanofluid. 2009;7:751–6.
155. Zhu JJ, Xuan XC. Particle electrophoresis and dielectrophoresis in curved microchannels. J Colloid Interface Sci. 2009;340:285–90.
156. Zhu J, Xuan X. Curvature-induced dielectrophoresis for continuous separation of particles by charge in spiral microchannels. Biomicrofluidics. 2011;5:24111.
157. DuBose J, Lu X, Patel S, Qian S, Joo SW, Xuan X. Microfluidic electrical sorting of particles based on shape in a spiral microchannel. Biomicrofluidics. 2014;8:1–8.
158. Kale A, Malekanfard A, Xuan X. Analytical guidelines for designing curvature-induced dielectrophoretic particle manipulation systems. Micromachines. 2020;11:707.
159. Kale A, Malekanfard A, Xuan X. Curvature-induced dielectrophoretic particle manipulation systems. Micromachines. 2020;11:707.
160. Zhu J, Canter RC, Keten G, Vedantam P, Tzeng T-RRJ, Xuan X. Continuous-flow particle and cell separations in a serpentine microchannel via curvature-induced dielectrophoresis. Microfluid Nanofluid. 2011;11:743–52.
161. Li M, Li S, Li W, Wen W, Alici G. Continuous manipulation and separation of particles using combined obstacle- and curvature-induced direct current dielectrophoresis. Electrophoresis. 2013;34:952–60.
162. Ying LM, White SS, Bruckbauer A, Meadows L, Korchev YE, Klenerman D. Frequency and voltage dependence of the dielectrophoretic trapping of short lengths of DNA and dCTP in a nanopipette. Biophys J. 2004;86:1018–27.
163. Clarke RW, White SS, Zhou D, Ying L, Klenerman D. Trapping of proteins under physiological conditions in a nanopipette. Angew Chem Int Ed. 2005;44:3747–50.
164. Clarke RW, Piper JD, Ying L, Klenerman D. Surface conductivity of biological macromolecules measured by nanopipette dielectrophoresis. Phys Rev Lett. 2007;98:198102.1–4.
165. Shi L, Rana A, Esfandiari L. A low voltage nanopipette dielectrophoretic device for rapid entrapment of nanoparticles and exosomes extracted from plasma of healthy donors. Sci Rep. 2018;8:6751.
166. Shi L, Kuhnell D, Borra VJ, Langevin SM, Nakamura T, Esfandiari L. Rapid and label-free isolation of small extracellular vesicles from biofluids utilizing a novel insulator based dielectrophoretic device. Lab Chip. 2019;19:3726–34.
167. Jones PV, DeMichele AF, Kemp LK, Hayes MA. Differentiation of *Escherichia coli* serotypes using DC gradient insulator dielectrophoresis. Anal Bioanal Chem. 2014;406:183–92.
168. Cho Y-KK, Kim S, Lee K, Park C, Lee J-GG, Ko C. Bacteria concentration using a membrane type insulator-based dielectrophoresis in a plastic chip. Electrophoresis. 2009;30:3153–9.
169. Mukaibo H, Wang T, Perez-Gonzalez VH, Getpreecharsawas J, Wurzer J, Lapizco-Encinas BH, McGrath JL. Ultrathin nanoporous membranes for insulator-based dielectrophoresis. Nanotechnology. 2018;29:235704 (10pp).
170. Suehiro J, Zhou GB, Imamura M, Hara M. Dielectrophoretic filter for separation and recovery of biological cells in water. IEEE Trans Ind Appl. 2003;39:1514–21.
171. Jun S, Chun C, Ho K, Li Y. Design and evaluation of a millifluidic insulator-based dielectrophoresis (DEP) retention device to separate bacteria from tap water. Water. 2021;13:1678.
172. Baylon-Cardiel JL, Lapizco-Encinas BH, Reyes-Betanzo C, Chávez-Santoscoy AV, Martínez-Chapa SO. Prediction of trapping zones in an insulator-based dielectrophoretic device. Lab Chip. 2009;9:2896–901.
173. Jesús-Pérez NM, Lapizco-Encinas BH. Dielectrophoretic monitoring of microorganisms in environmental applications. Electrophoresis. 2011;32:2331–57.
174. Gallo-Villanueva RC, Pérez-González VH, Davalos RV, Lapizco-Encinas BH. Separation of mixtures of particles in a multipart microdevice employing insulator-based dielectrophoresis. Electrophoresis. 2011;32:2456–65.
175. Hill N, Lapizco-Encinas BH. On the use of correction factors for the mathematical modeling of insulator based dielectrophoretic devices. Electrophoresis. 2019;40:2541–52.
176. Kwon JS, Maeng JS, Chun MS, Song S. Improvement of microchannel geometry subject to electrokinesis and dielectrophoresis using numerical simulations. Microfluid Nanofluid. 2008;5:23–31.
177. M. KS, Dukhin SS, Vidov OI. Aperiodic electrophoresis. Colloid J. 1994;56:579–85.
178. Voldman J. Electrical forces for microscale cell manipulation. Annu Rev Biomed Eng. 2006;8:425–54.
179. Hilton SH, Hayes MA. A mathematical model of dielectrophoretic data to connect measurements with cell properties. Anal Bioanal Chem. 2019;411:2223–37.
180. Miller A, Hill N, Hakim K, Lapizco-Encinas BH. Fine-tuning electrokinetic injections considering nonlinear electrokinetic effects in insulator-based devices. Micromachines 2021. 2021;12:628.